Anisotropic Mach Cone Aligned Mesh Adaptation for Low Boom Simulations

Chase Ashby, Jeffrey Housman, Jared Duensing

Computational Aerosciences Branch

Advanced Modeling & Simulation (AMS) Seminar Series

NASA Ames Research Center, July 6th, 2023

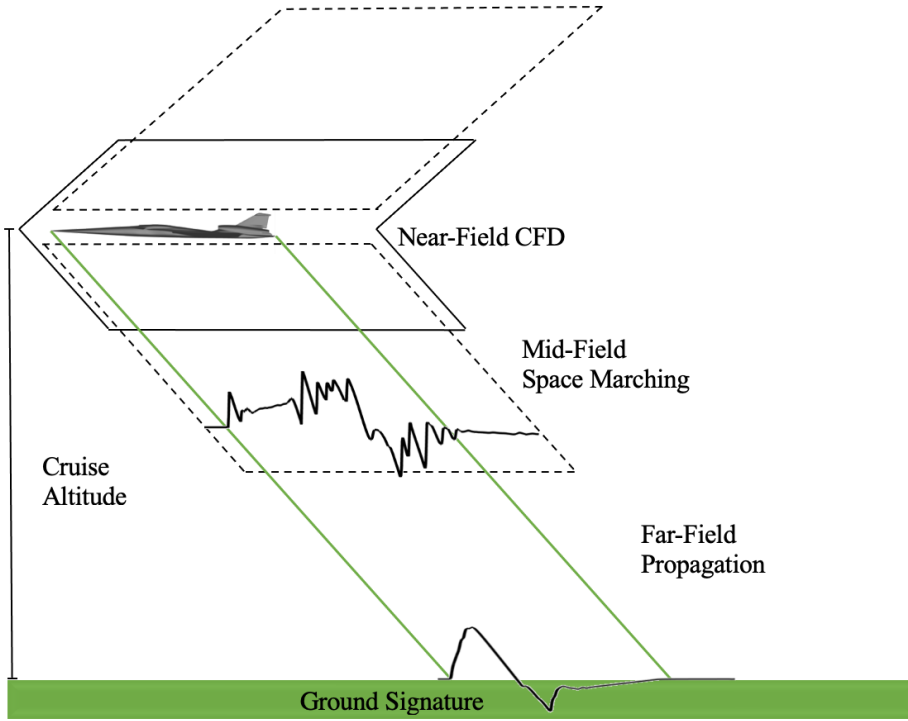
This material is a work of the U.S. Government and is not subject to copyright protection in the United States.

Outline

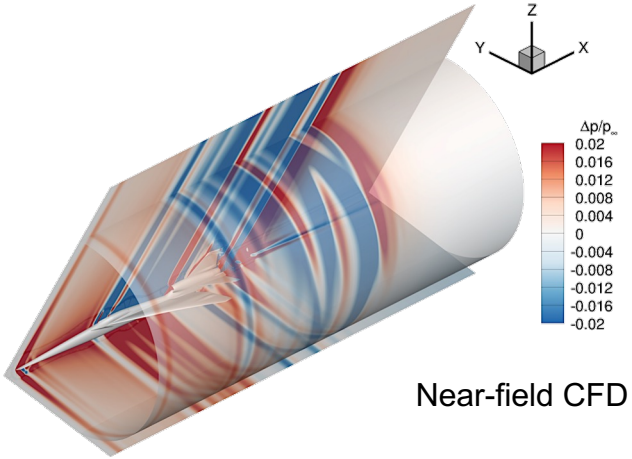
- Introduction
- Adaptation Methodology
  - Overset grid system
  - Adaptation equations
  - Direction-based error indicators
- Results
  - JAXA Wing Body
  - X-59 C608 Demonstrator Model
- Summary

Motivation

- Evaluation of low boom aircraft designs rely on accurate predictions of ground-level noise
- Mission planning requires a large database consisting of O(1,000) – O(10,000) solutions
  - Must be accurate
  - Must be automated
- The Launch, Ascent, and Vehicle Aerodynamics (LAVA) framework uses a three-step prediction procedure
- Near-field CFD dominates the simulation cost

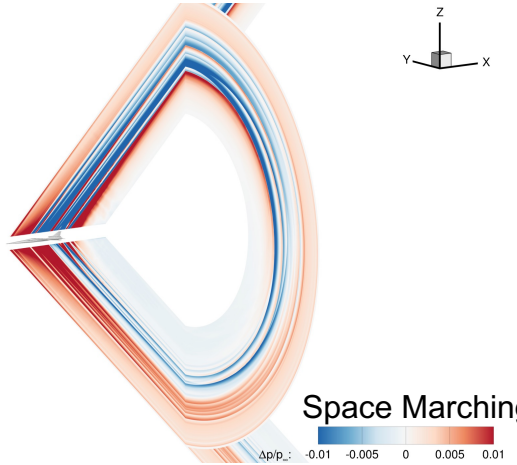


Low Boom Simulation Procedure

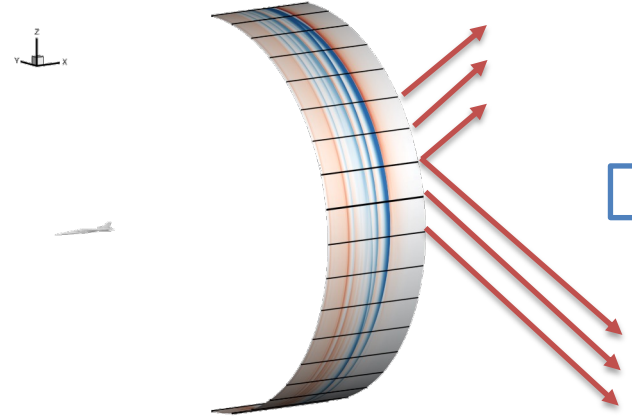


Near-field CFD

Interpolation
+
Space Marching

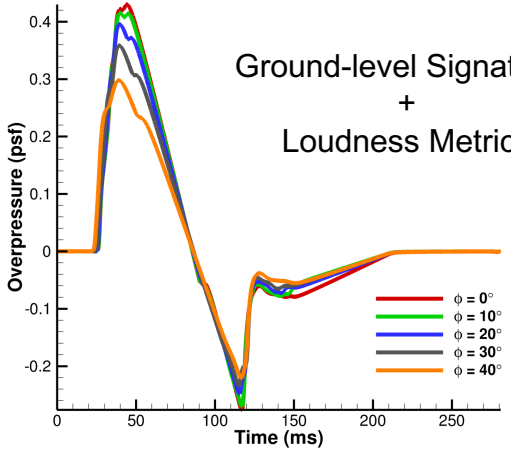


Space Marching



Pressure Cylinder Extraction

Acoustic Propagation

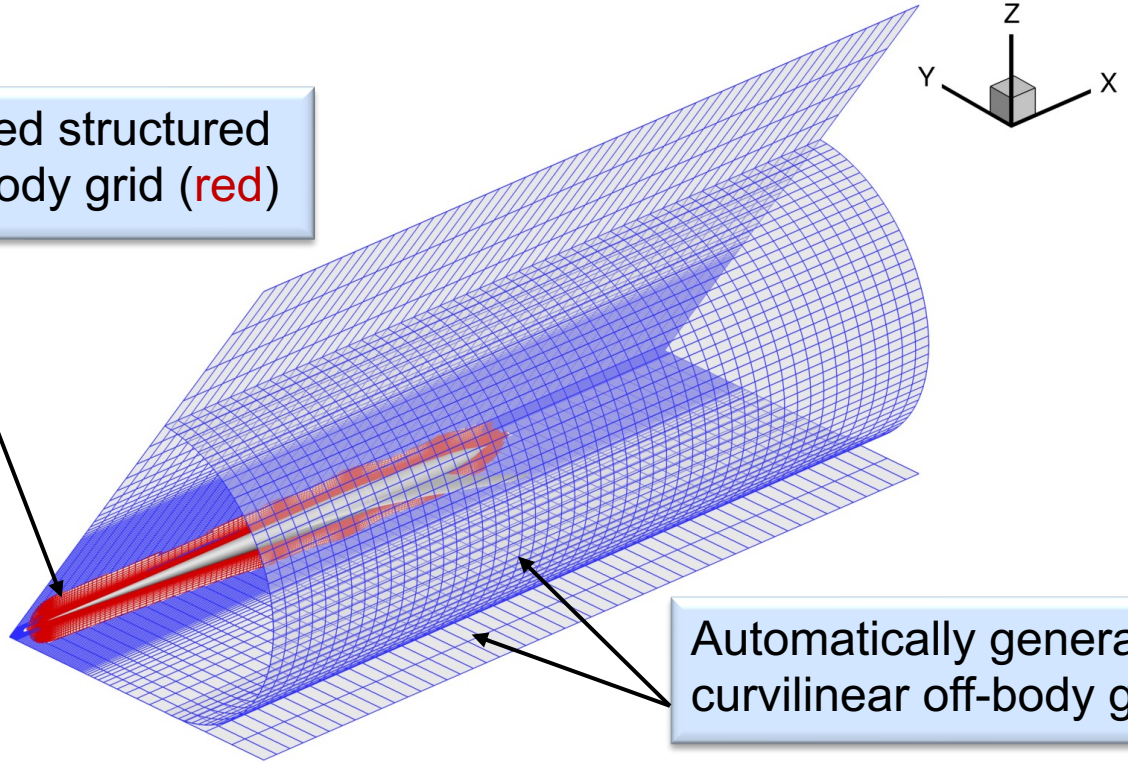


Ground-level Signatures
+
Loudness Metrics

Objectives

- Automate the off-body grid generation procedure for near-field simulations
  - Increase robustness to flight plan changes
- Generate improved CFD grid system with fixed degrees of freedom
  - Reduce resource requirements for achievable accuracy levels
- Construct error indicators to facilitate rapid anisotropic mesh adaptation
  - Capture error for complex shock-dominated supersonic flows

Overset Grid System

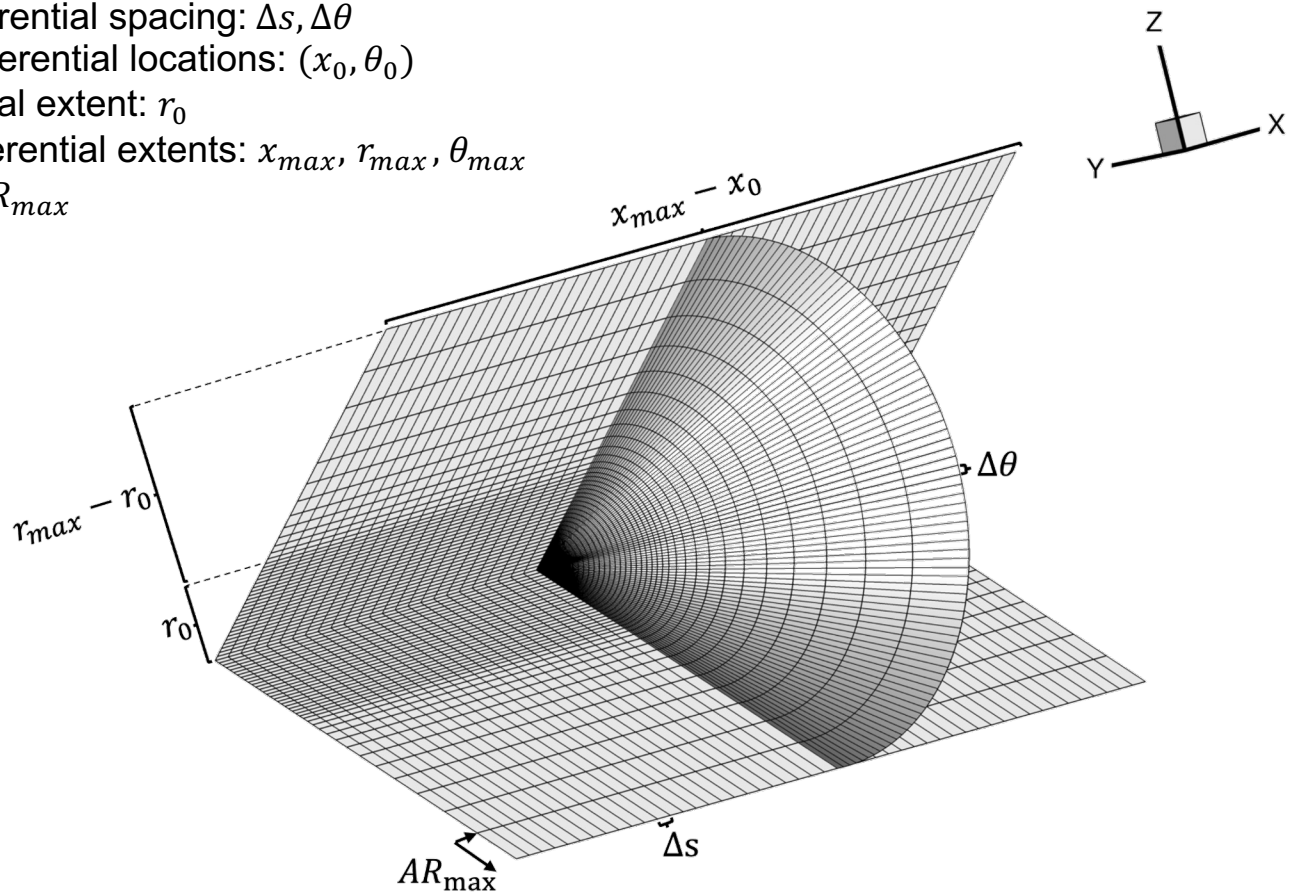


Manually generated structured curvilinear near-body grid (red)

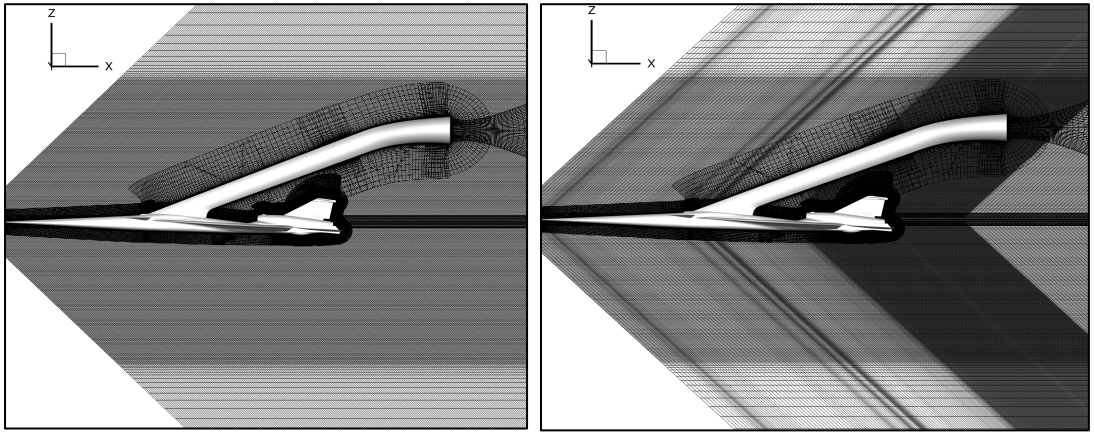
Automatically generated structured curvilinear off-body grid (blue)

Mach Cone Aligned Off-Body CFD Grid

- Streamwise and circumferential spacing: $\Delta s, \Delta\theta$
- Starting axial and circumferential locations: (x_0, θ_0)
- Near-body resolution radial extent: r_0
- Axial, radial, and circumferential extents: x_{max}, r_{max}, θ_{max}
- Maximum aspect ratio: AR_{max}
- Stretching ratio: SR

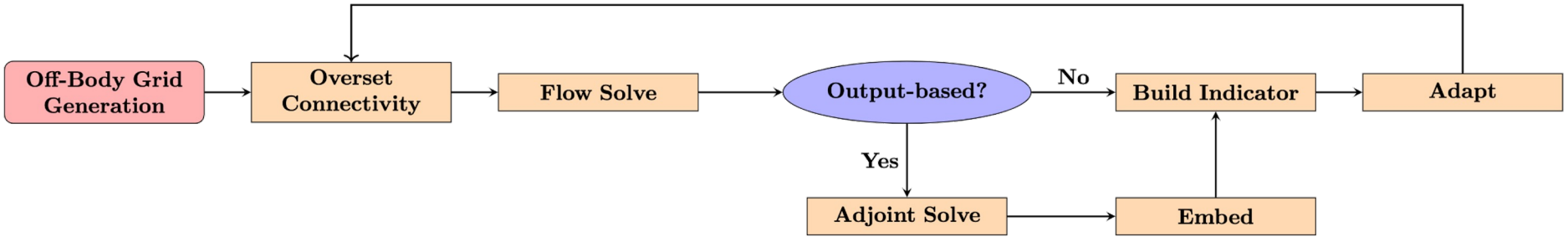


Adaptation Process



Initial Off-body

Adapted Grid



Adaptation Equations

- Direction-based mesh redistribution is governed by the equation

$$w_i \underbrace{\Delta s_i}_{\text{cell-size}} = C$$

Discrete equidistribution principle

- Adaptation weights control the location of local refinement

$$w_i = 1 + A \underbrace{f_i}_{\text{error indicator}}$$

- Clustering constant limits the maximum and minimum cell-size

$$A = \underbrace{c_{\mathrm{f}} r_{\mathrm{f}}}_{\text{coarsening and refinement factors}} \frac{\Delta s^0_{\max}}{\Delta s^0_{\min}} - 1$$

Error Indicators

Feature-based Indicators

- **Target errors in specific flow quantities**

$$q = \text{Mach, pressure disturbance, etc.}$$

- **Relies on second undivided difference**

$$e_i = |q_{i+1} - 2\,q_i + q_{i-1}|$$

- **Non-dimensional and direction independent**

$$e(\xi_j, \eta_k, \zeta_l) = \max_{i=j,k,l} \frac{|q_{i+1} - 2q_i + q_{i-1}|}{q_{\text{ref}}}$$

Output-based Indicators

- **Target errors in single or multiple scalar output quantities of interest**

$$\varepsilon = |J(\mathbf{Q}) - J_{\text{H}}(\mathbf{Q}_{\text{H}})|$$

where

$$J(\mathbf{Q}) = \int_0^L \left(\frac{\Delta p}{p_\infty}\right)^2 ds$$

- **Output-based Indicator on embedded grid**

$$e_{\text{h}} = \left(\boldsymbol{\psi}_{\text{h}}^{\text{HI}} - \boldsymbol{\psi}_{\text{h}}^{\text{LO}}\right)^T \mathbf{R}_{\text{h}}(\mathbf{Q}_{\text{h}}^{\text{LO}})$$

Pieter G. Buning and Thomas H. Pulliam. "Near-Body Grid Adaption for Overset Grids," AIAA 2016-3326. *46th AIAA Fluid Dynamics Conference*. June 2016.

Error Indicators

Output-based Indicators

- **Target errors in single or multiple scalar output quantities of interest**

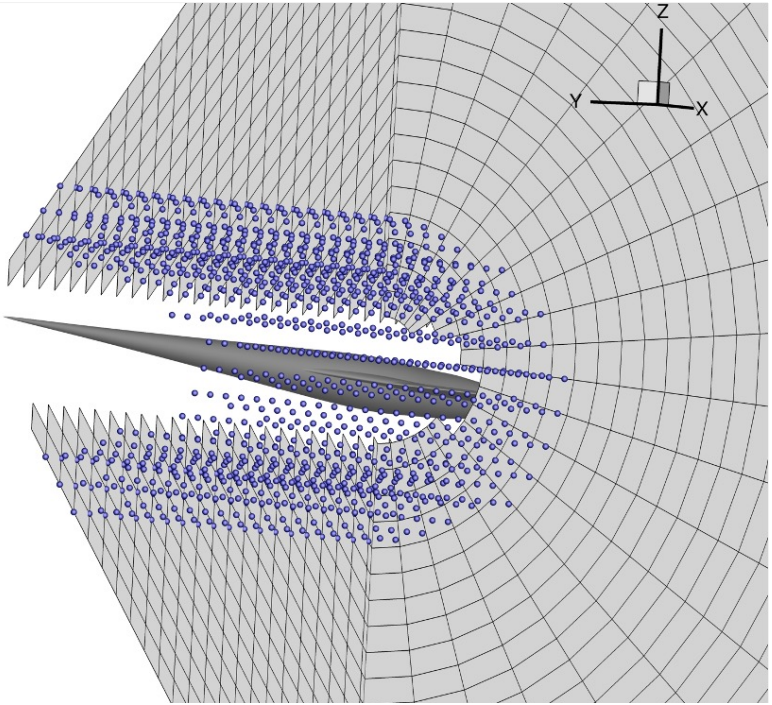
$$\varepsilon = \left| J(\mathbf{Q}) - J_{\mathrm{H}}(\mathbf{Q}_{\mathrm{H}}) \right|$$

where

$$J(\mathbf{Q}) := \sum_{i=1}^{N_{\mathrm{fringe}}} \left(\frac{\Delta p_i}{p_\infty} \right)^2$$

- **Output-based Indicator on embedded grid**

$$e_{\mathrm{h}} = \left(\boldsymbol{\psi}_{\mathrm{h}}^{\mathrm{HI}} - \boldsymbol{\psi}_{\mathrm{h}}^{\mathrm{LO}} \right)^T \mathbf{R}_{\mathrm{h}}(\mathbf{Q}_{\mathrm{h}}^{\mathrm{LO}})$$



Space Marching Fringe Points

Direction-based Indicators

Four-step formulation procedure :

1) Streamwise indicator on a fixed radial surface ζ^*

$$g(\xi) = \max_{\eta} |e_0(\xi, \eta, \zeta^*)|$$

2) Applying a smoothing operator for low number of iterations

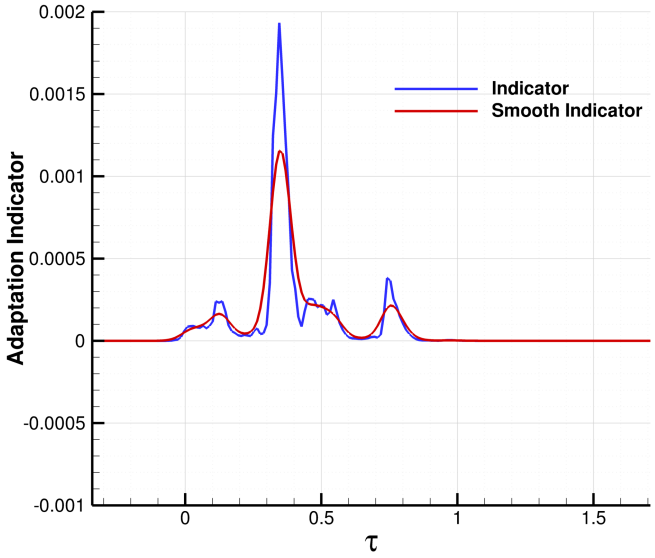
$$g_i^{\mathrm{s}} = \frac{g_{i-1} + 4g_i + g_{i+1}}{6}$$

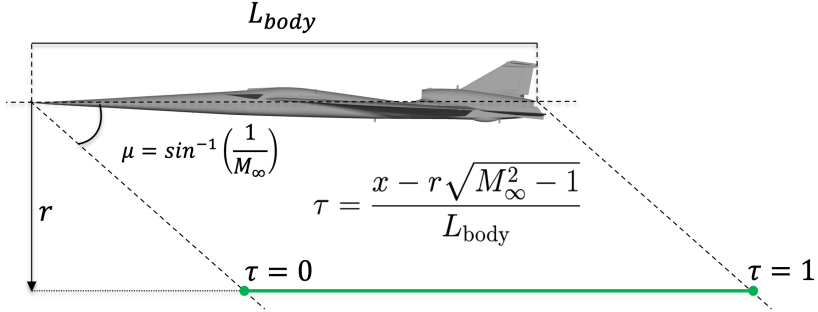
3) Map between [0,1) and form a surface indicator

$$f(\xi, \eta; \zeta^*) = \tanh(\beta\, g^{\mathrm{s}}(\xi)) \in [0, 1)$$

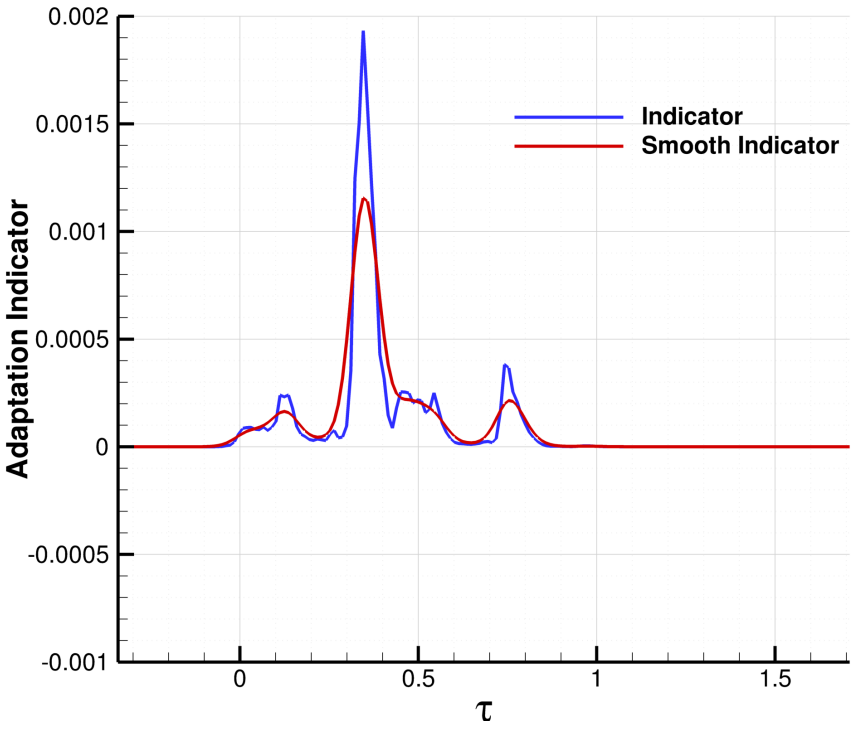
$$\beta = \tanh^{-1}(0.8)/(C\,\bar{g})$$

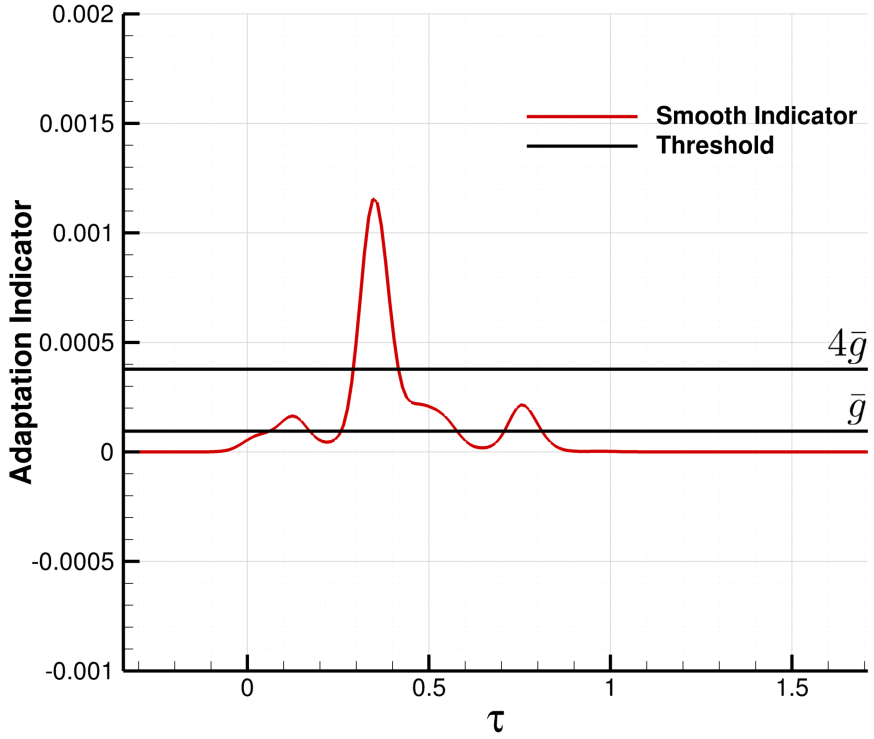
4) Interpolate to volume grid using normalized distance metric



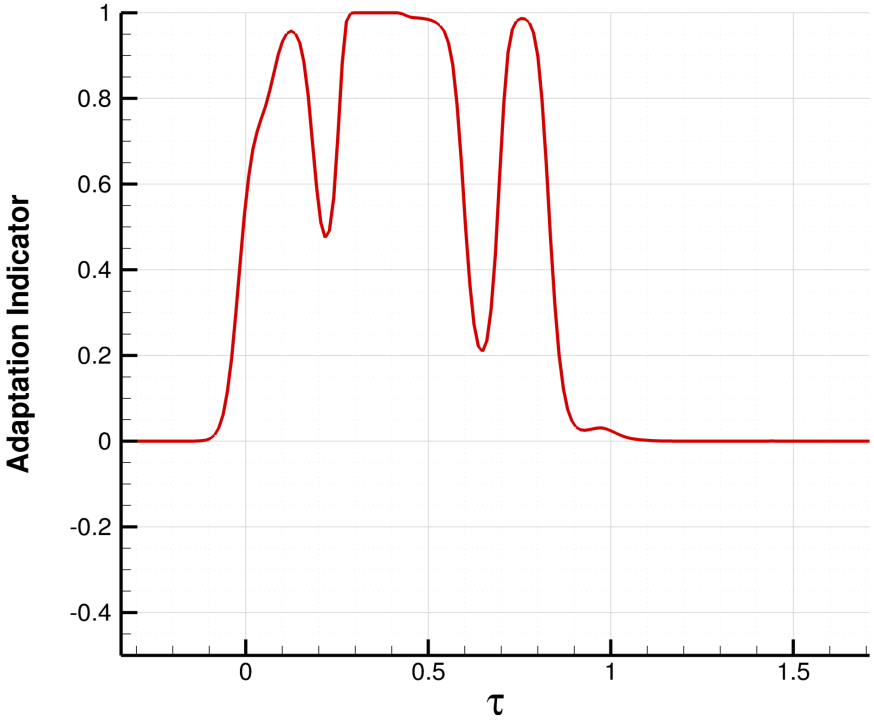


Direction-Based Indicator Mapping

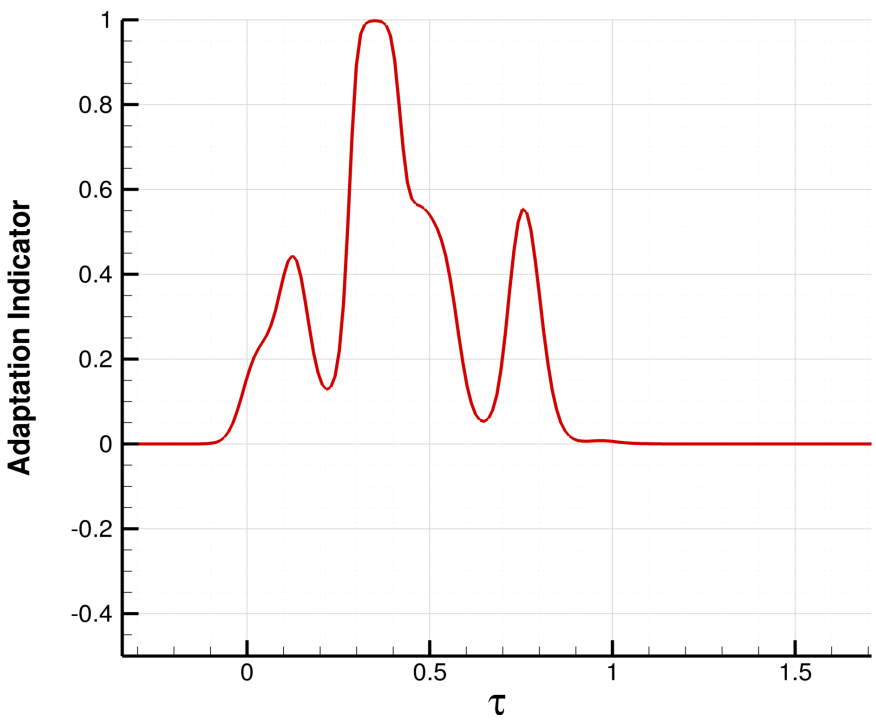




Direction-based Indicator Mapping

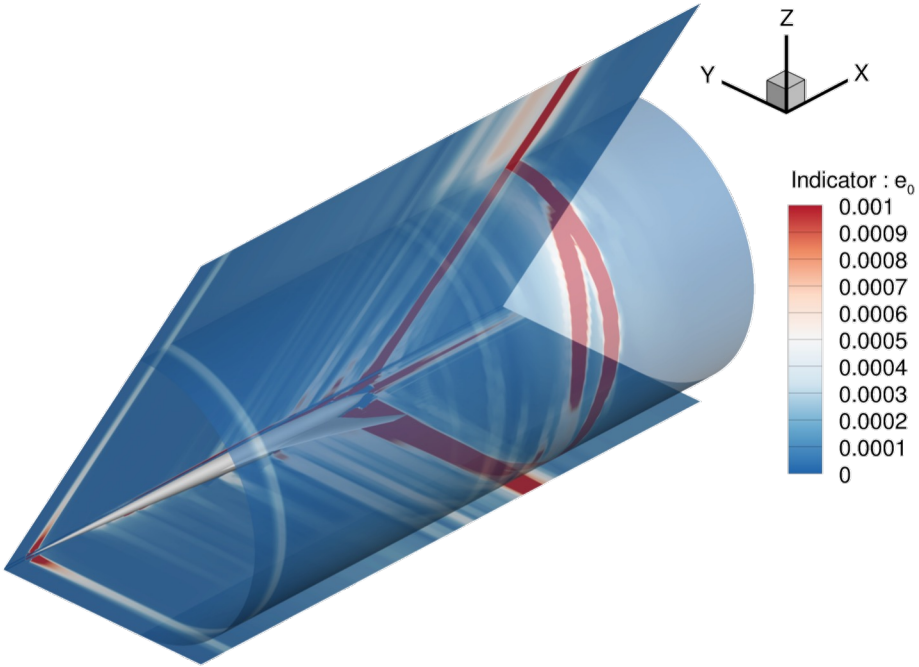


Final indicator using $\bar{g}$ threshold

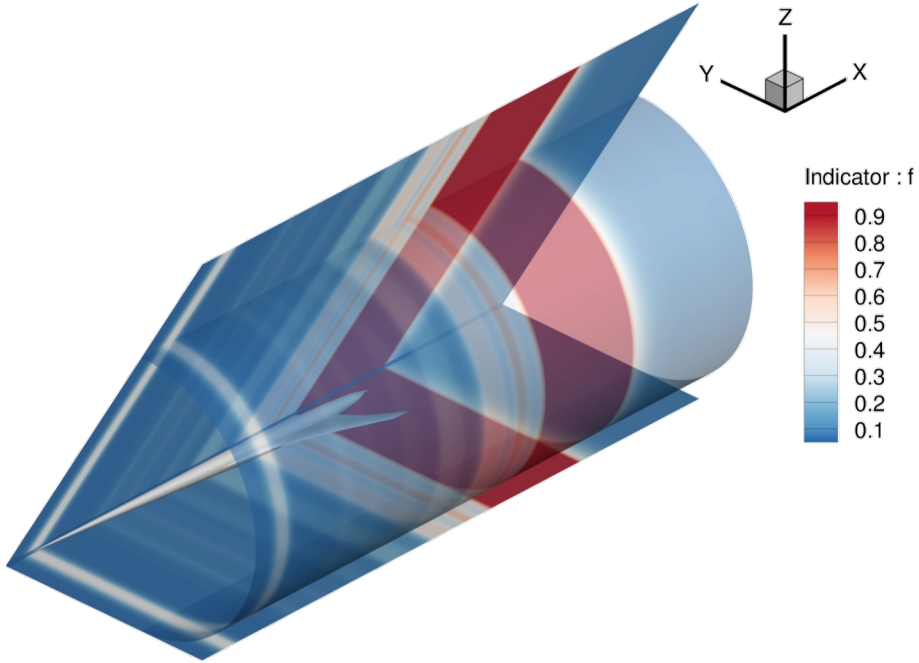


Final indicator using $4\bar{g}$ threshold

Direction-Based Indicators



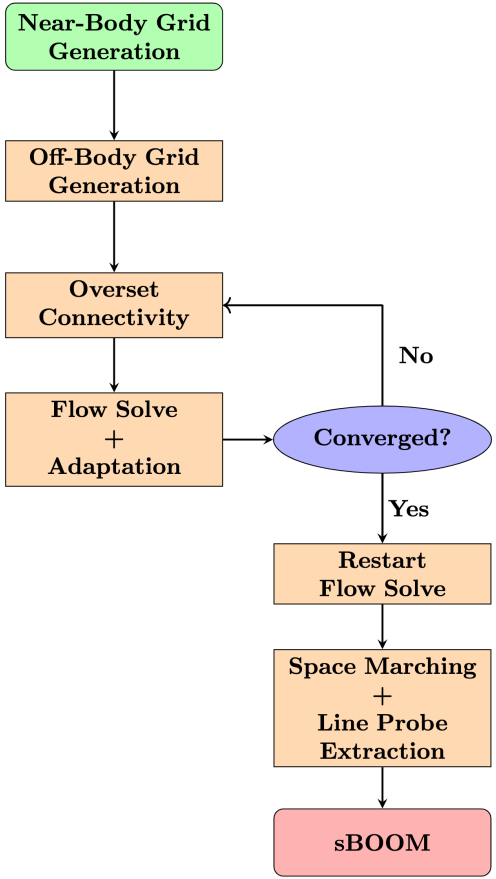
Initial Error Indicator



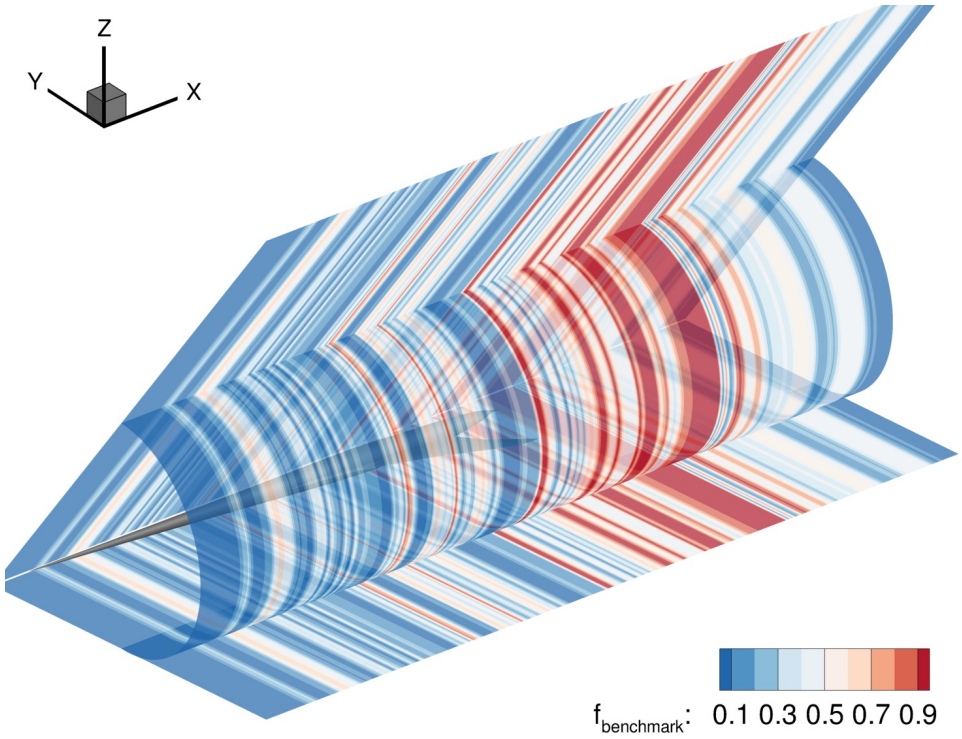
Final Direction-based Error Indicator

Results

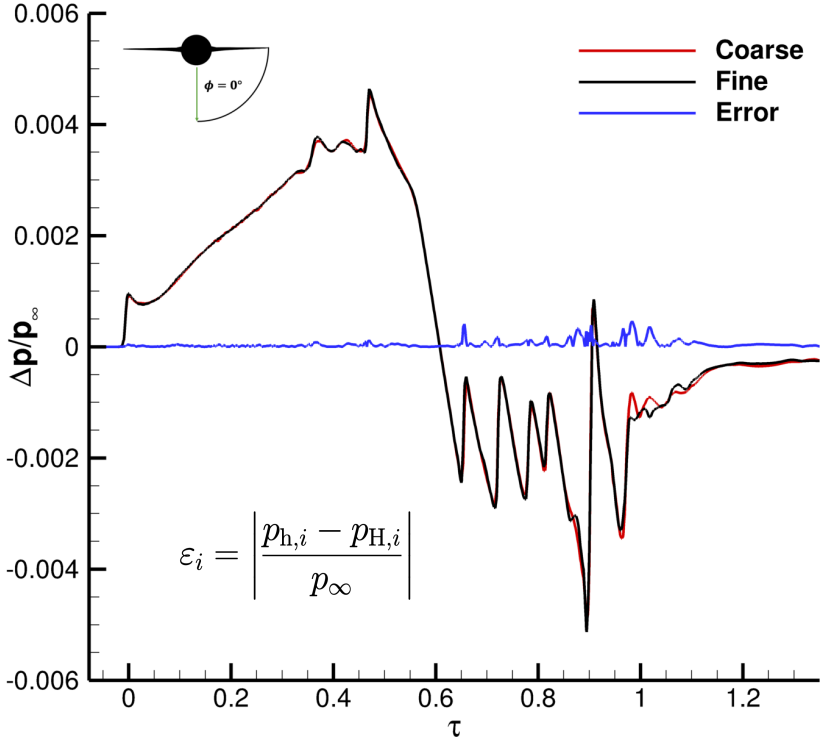
- Streamwise adapted and uniform off-body grids are compared for the entire prediction procedure
  - Uniform off-body grids have constant streamwise and circumferential spacing
- Near-body grids are held fixed for this study
  - Grid refinement studies performed during the 2nd and 3rd AIAA SBPWs
- The feature-based indicator is computed using Mach number as our flow quantity
- Loudness metrics:
  - A-weighted sound exposure level (ASEL)
  - B-weighted sound exposure level (BSEL)
  - C-weighted sound exposure kevel (CSEL)
  - Perceived loudness (PL)



Benchmark Indicator

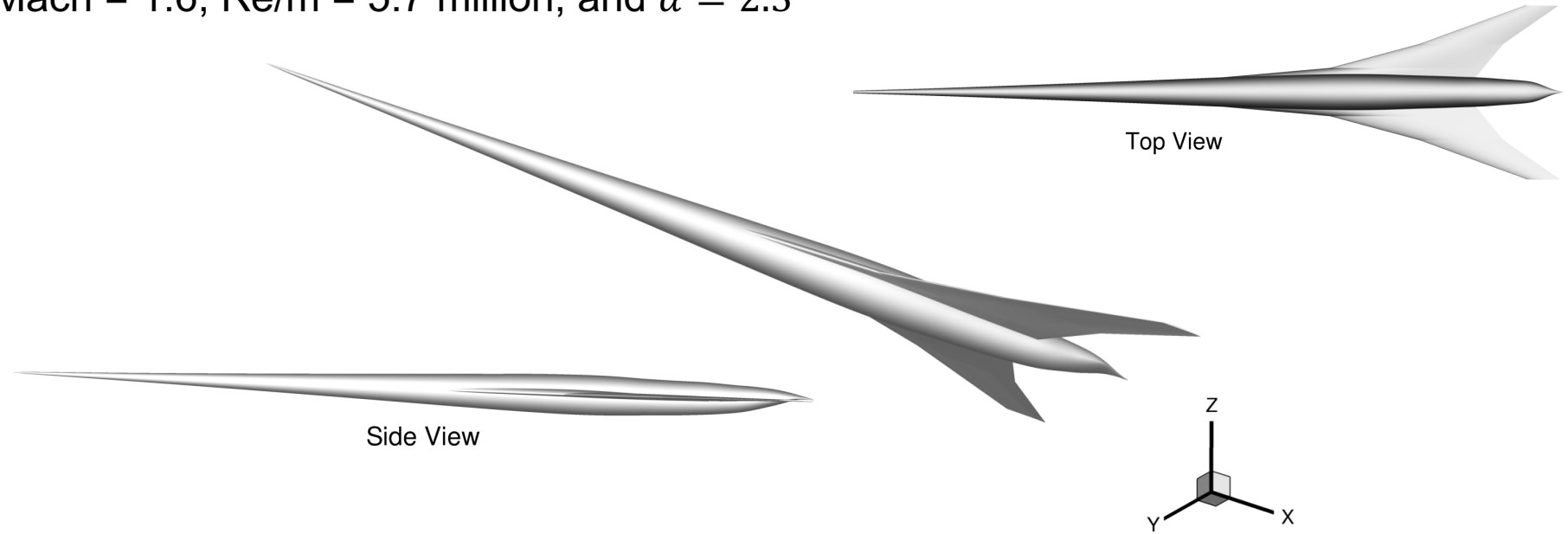


Benchmark Direction-Based Indicator

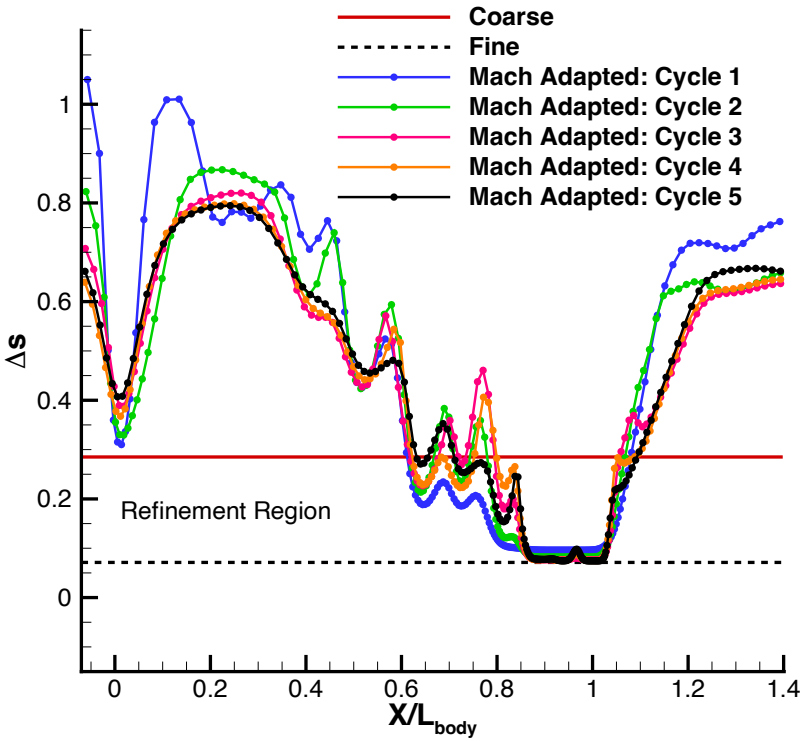


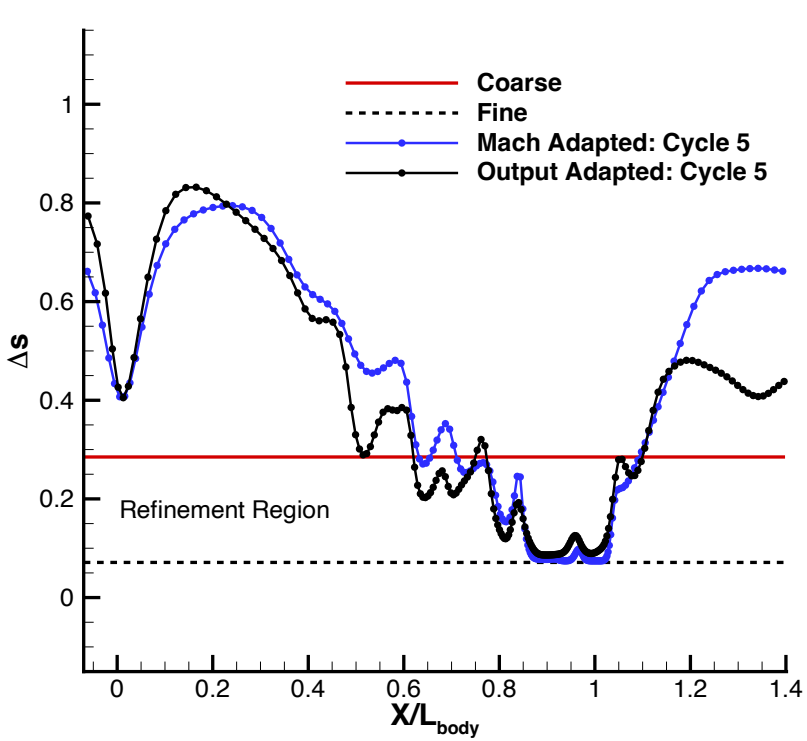
JAXA Wing Body

Reference length : $L_{ref} = 38.7\ m$
Cruise Altitude : 15,276 m
Mach = 1.6, Re/m = 5.7 million, and $\alpha = 2.3^{\circ}$

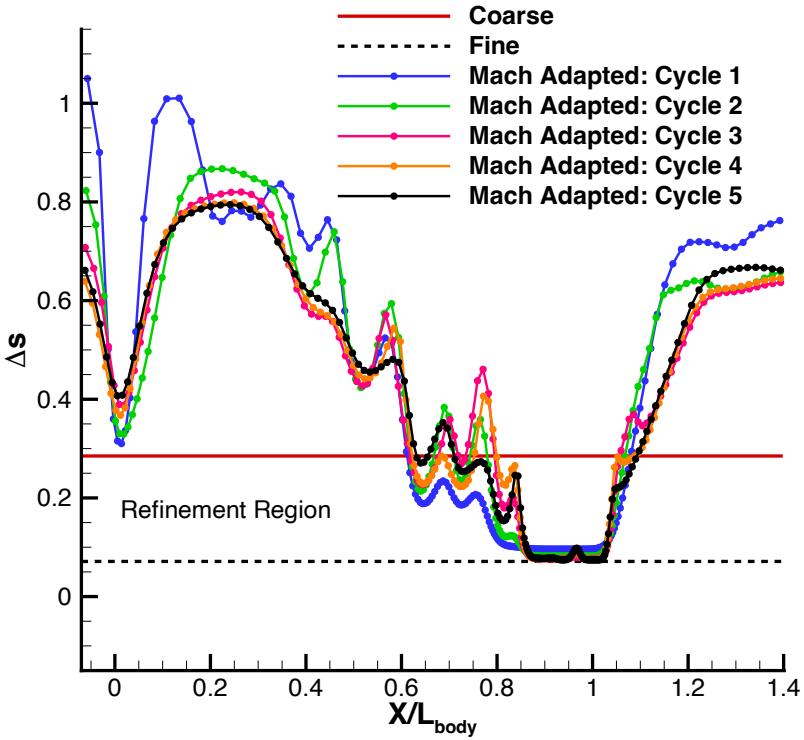


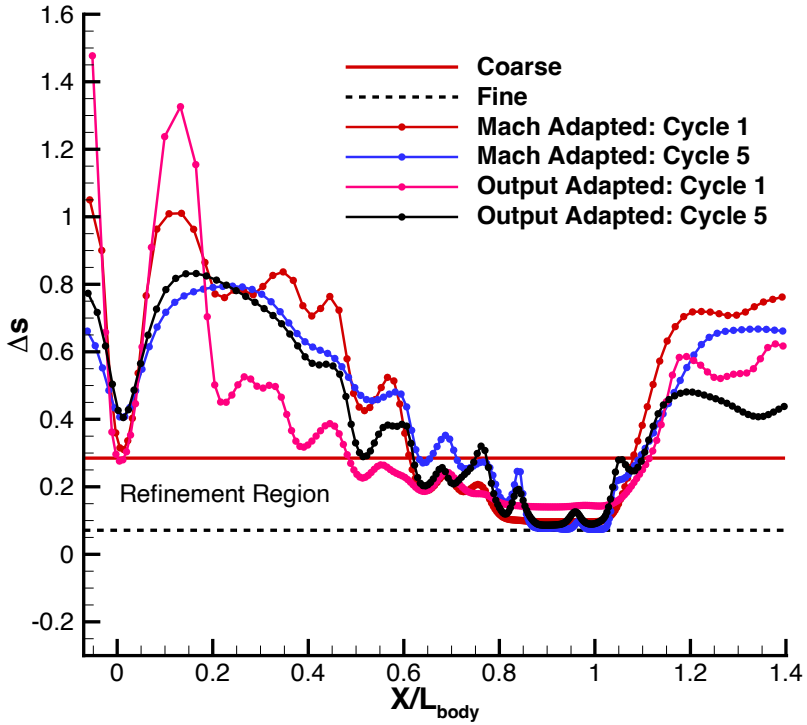
Cycle Convergence



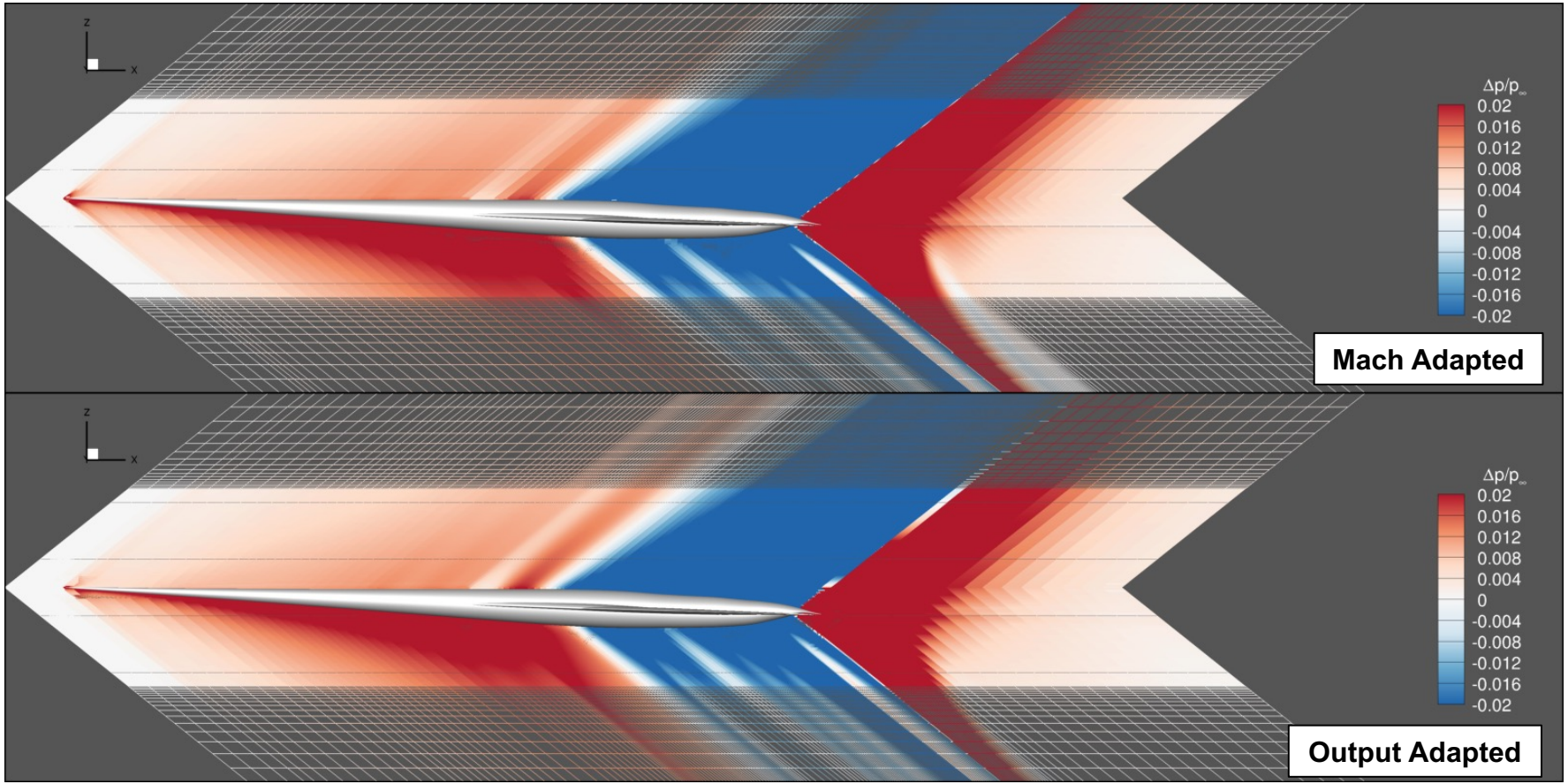


Cycle Convergence

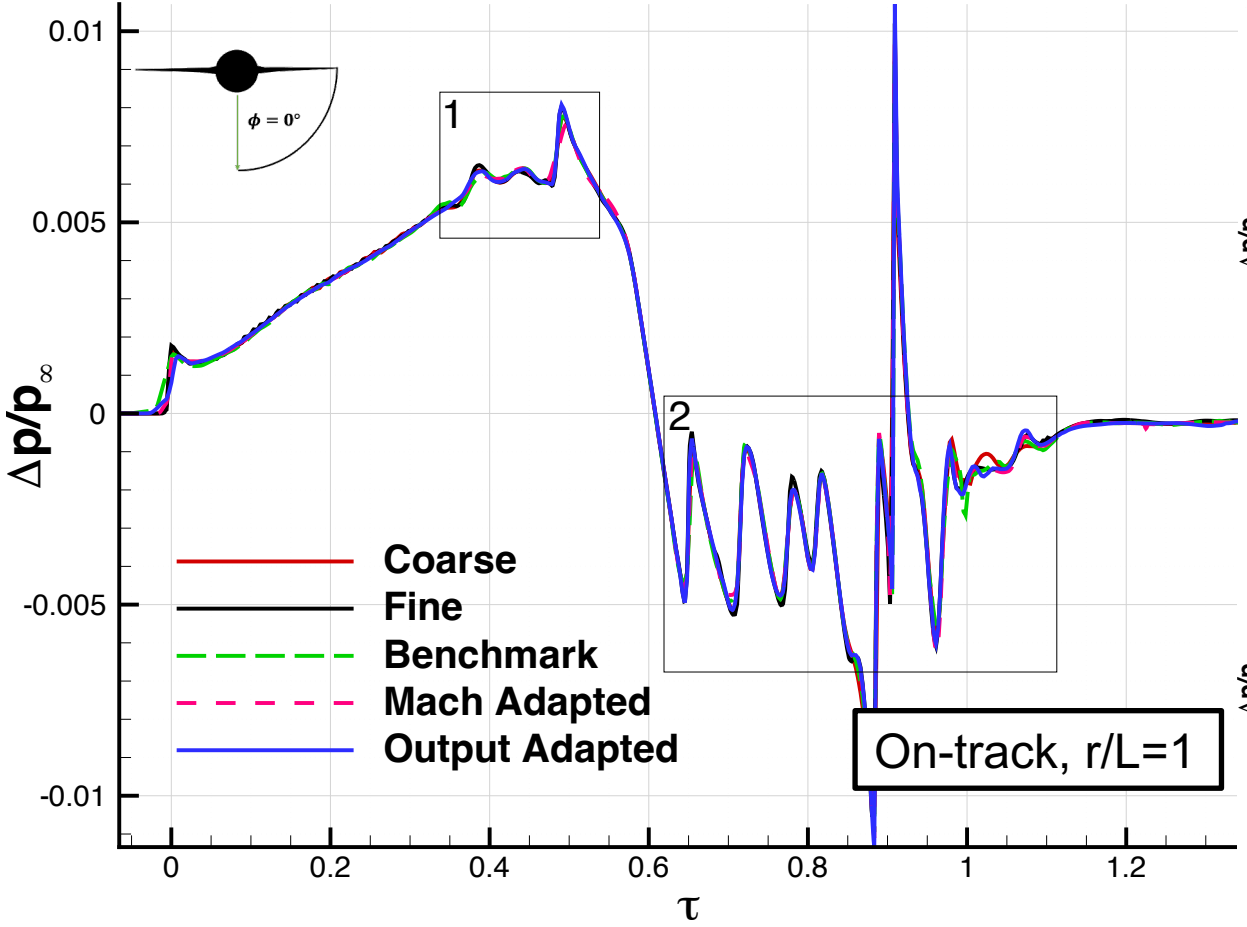


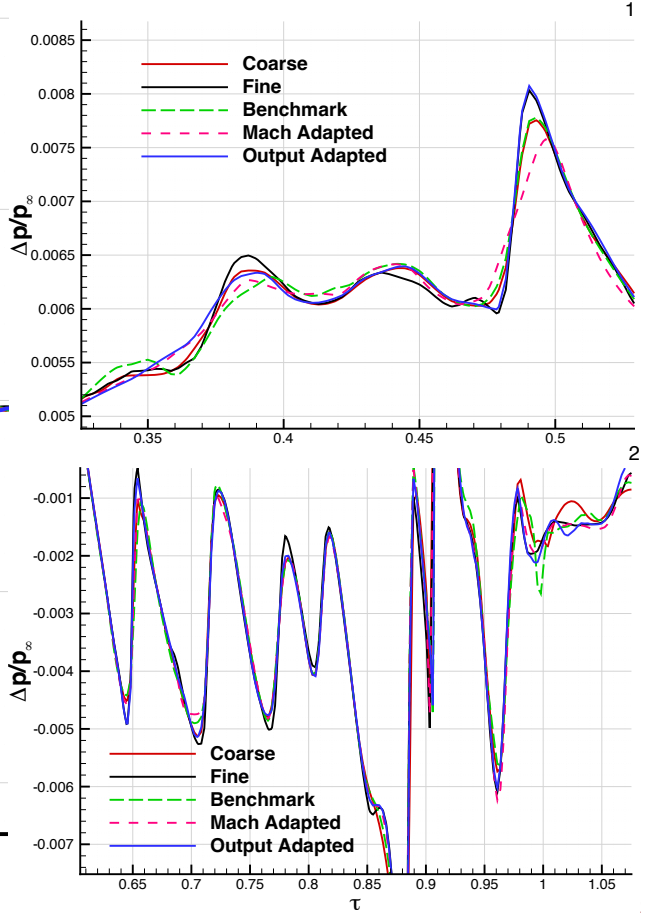


Streamwise Adapted Grids

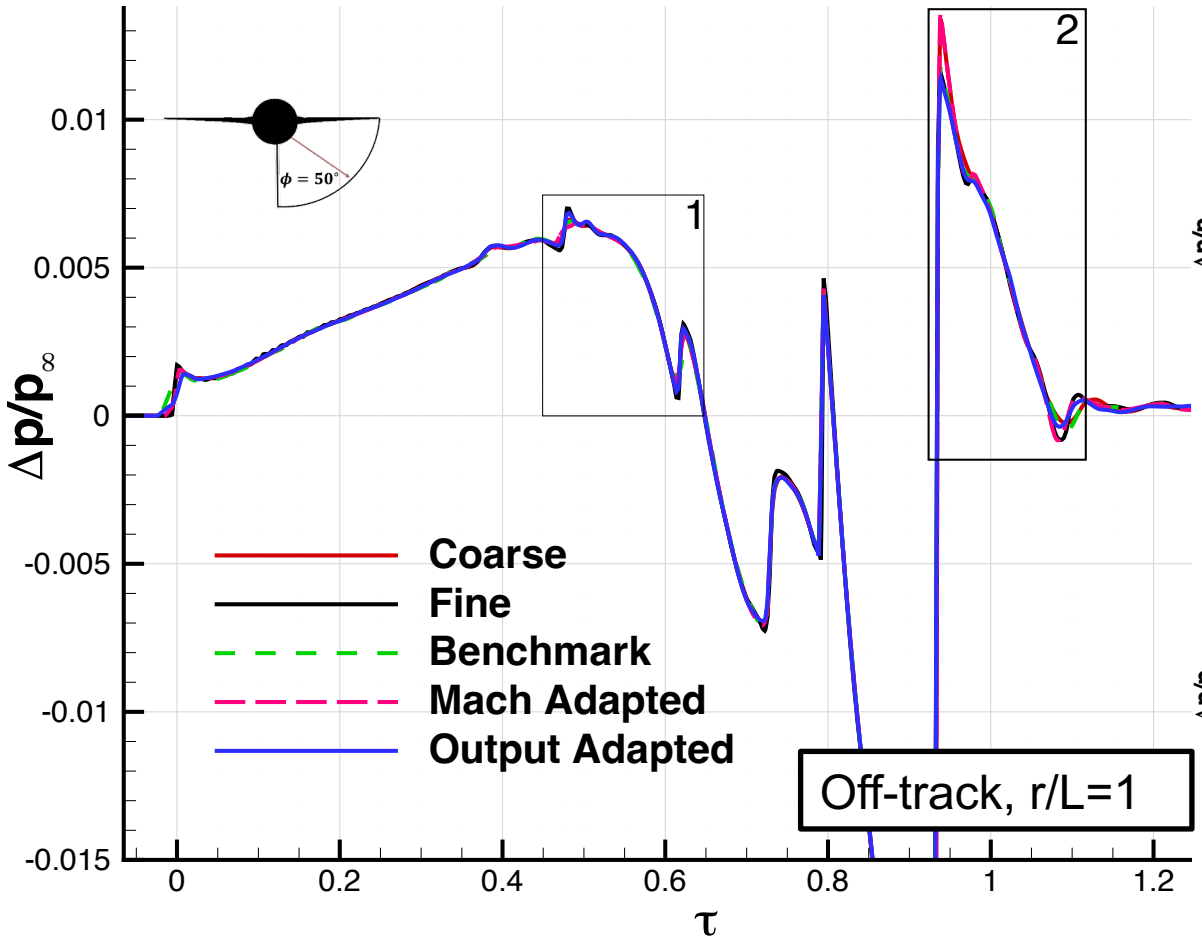


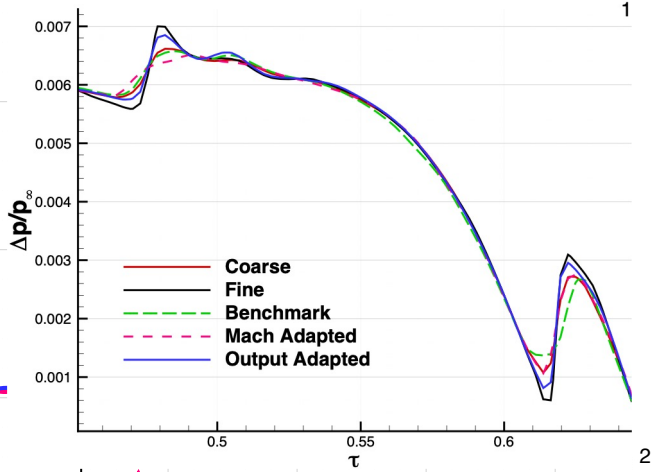
Near-field Accuracy Improvement

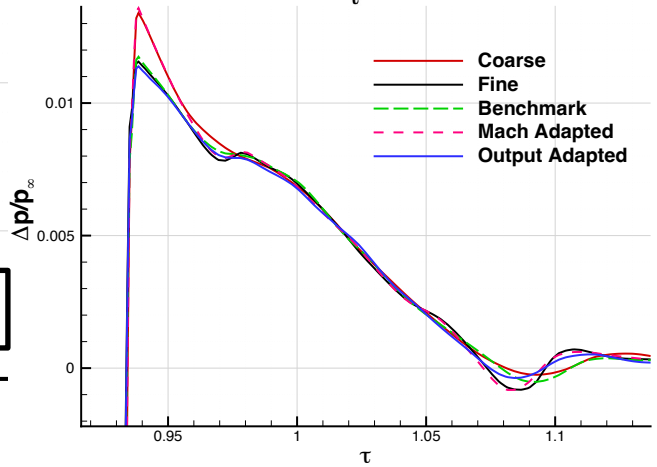




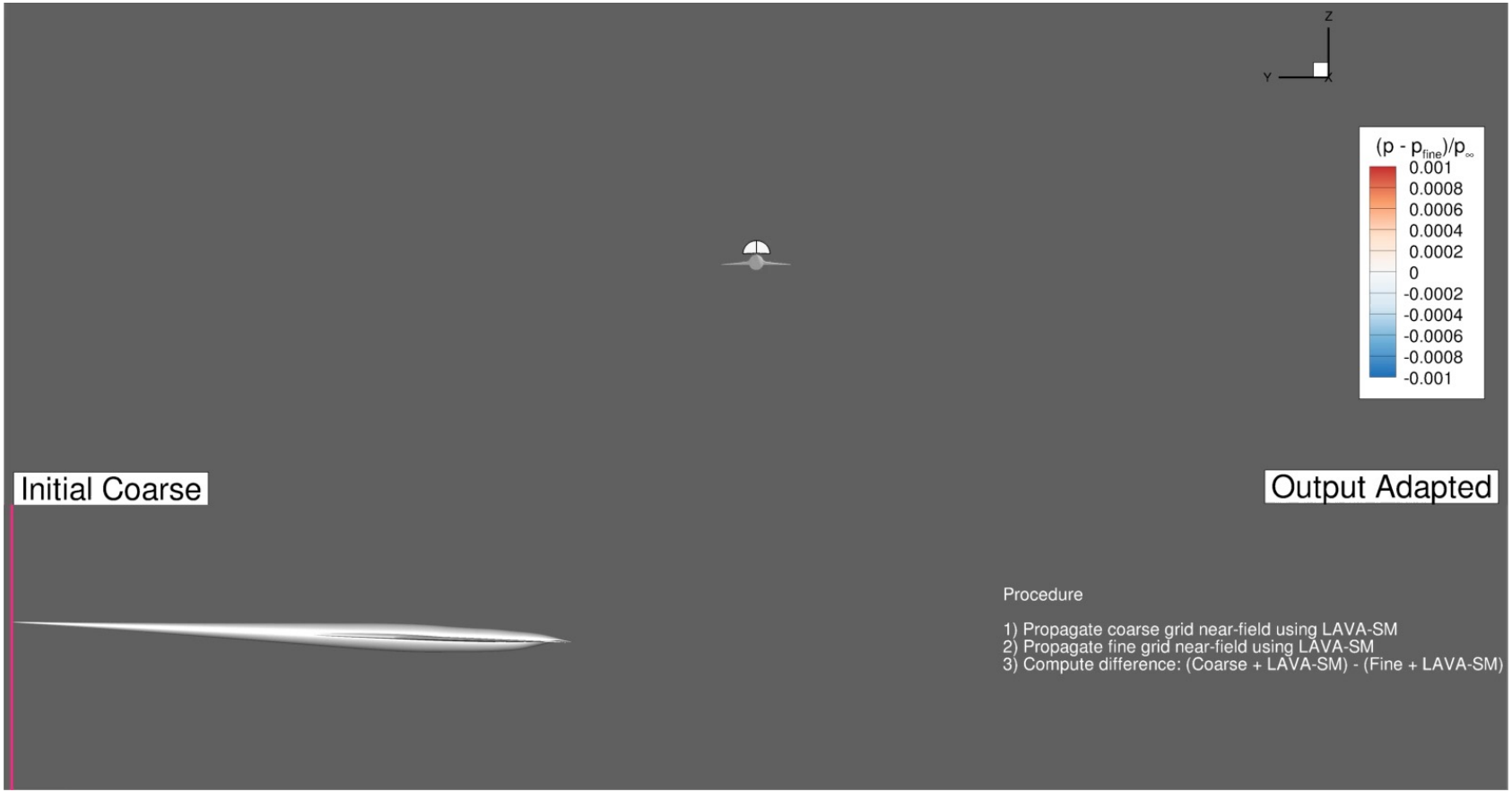
Near-field Accuracy Improvement



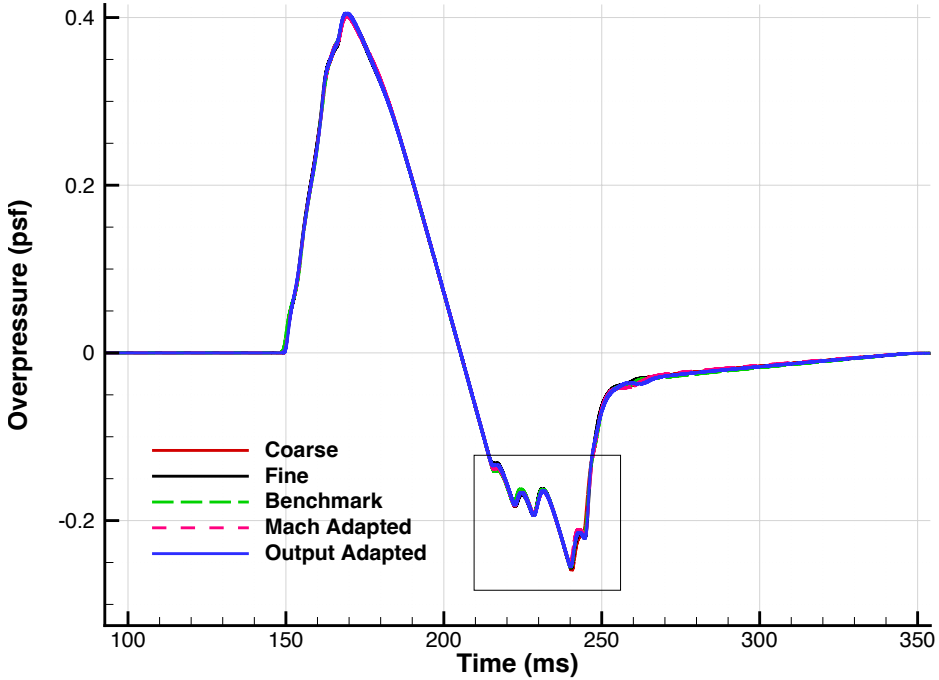


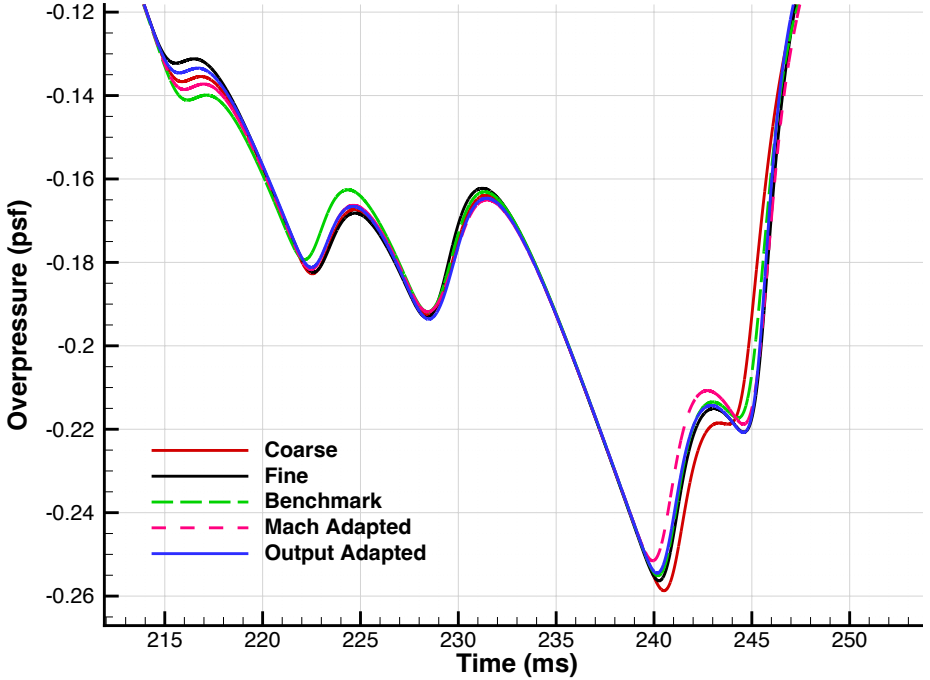


Near-field Propagation Difference



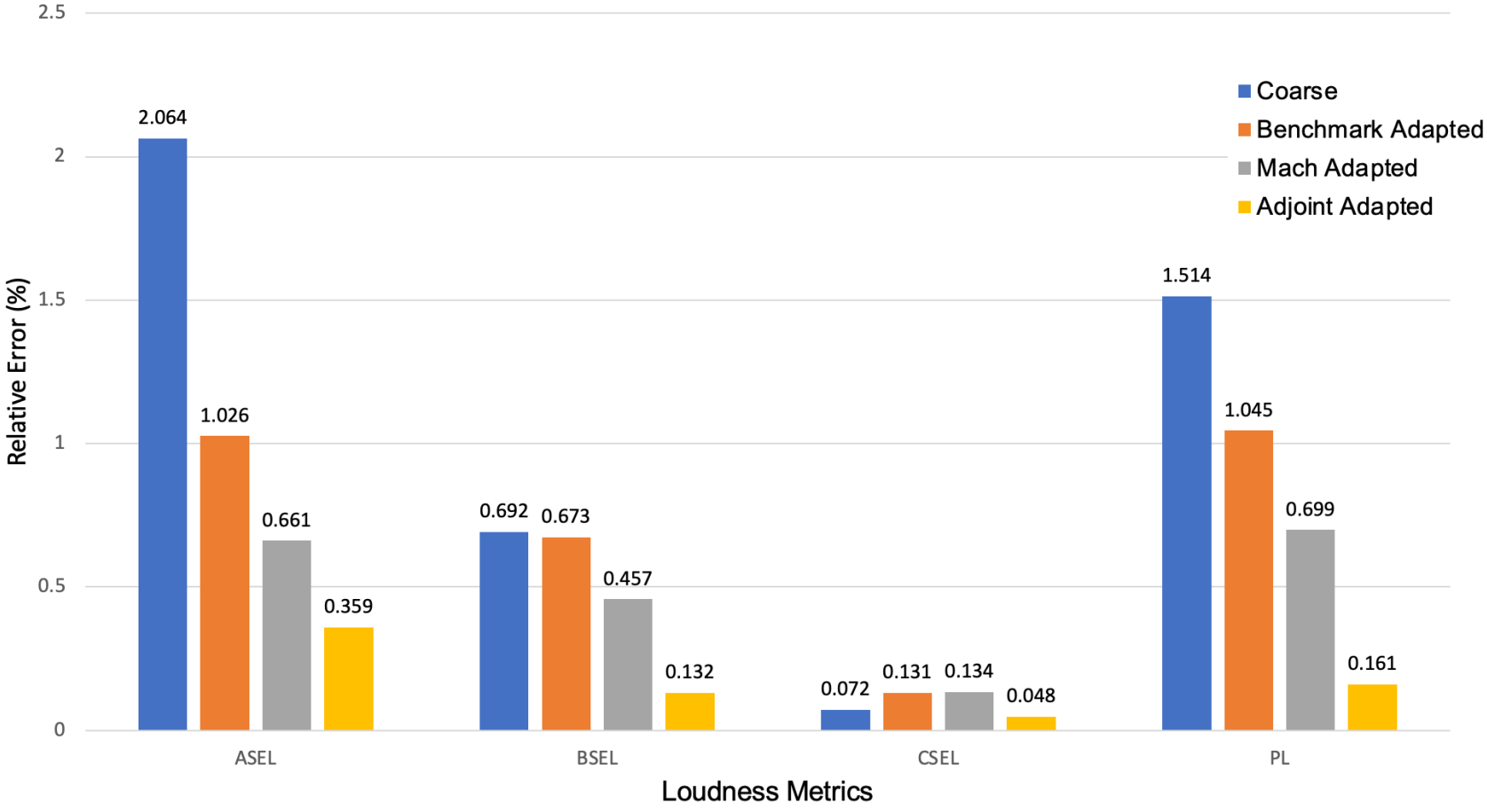
Ground-level Accuracy Improvements





Propagated on-track, r/L=3 pressure waveform

Ground Level Accuracy Improvement



Cost Analysis

Resource usage in CPU-hours for each JWB simulation performed on NASA's Electra supercomputer using five Skylake nodes, each containing two 20-core Xeon Gold 6148 sockets (2.4 GHz).

Grid	Connectivity	Primal Solve	Adjoint Solve	Embedding	Adaptation	Restart	**Total**
Coarse	0.14	25.46	-	-	-	-	**25.60**
Fine	0.13	55.99	-	-	-	-	**56.12**
Mach Adapted	0.29	25.46	-	-	0.01	5.66	**31.42**
Output Adapted	0.28	25.46	0.87	0.17	0.03	5.03	**31.56**

1.8x reduction in computational cost

X-59 C608 Demonstrator Model

Reference length : $L_{ref} = 27.432\ m$

Cruise Altitude : 16,215 m

Mach = 1.4, Re/m = 4.3 million, and $\alpha = 2.15^{\circ}$

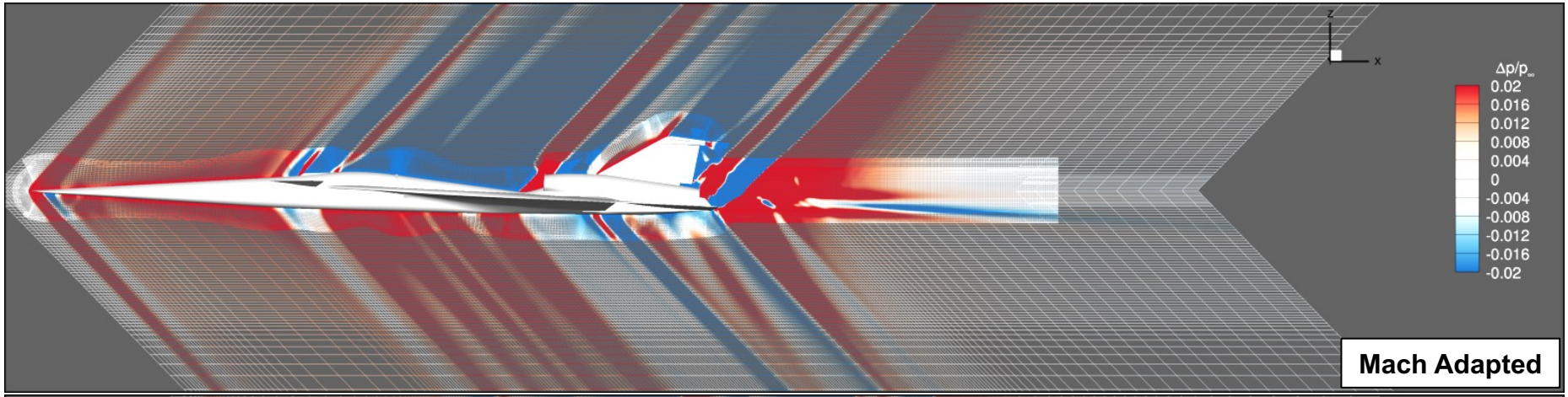


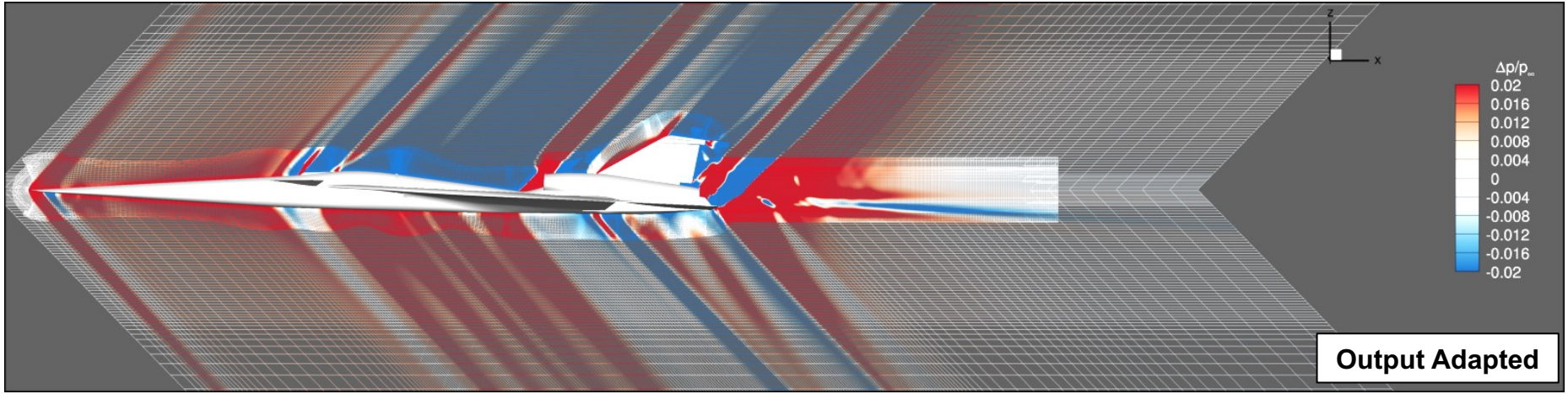
Front View



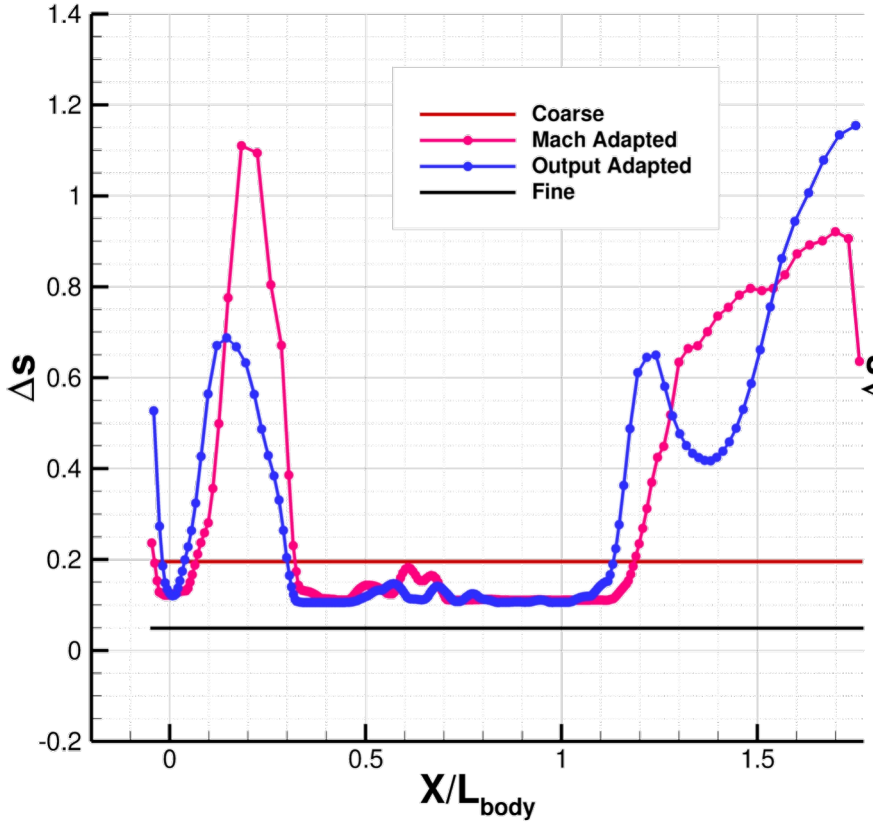
Side View

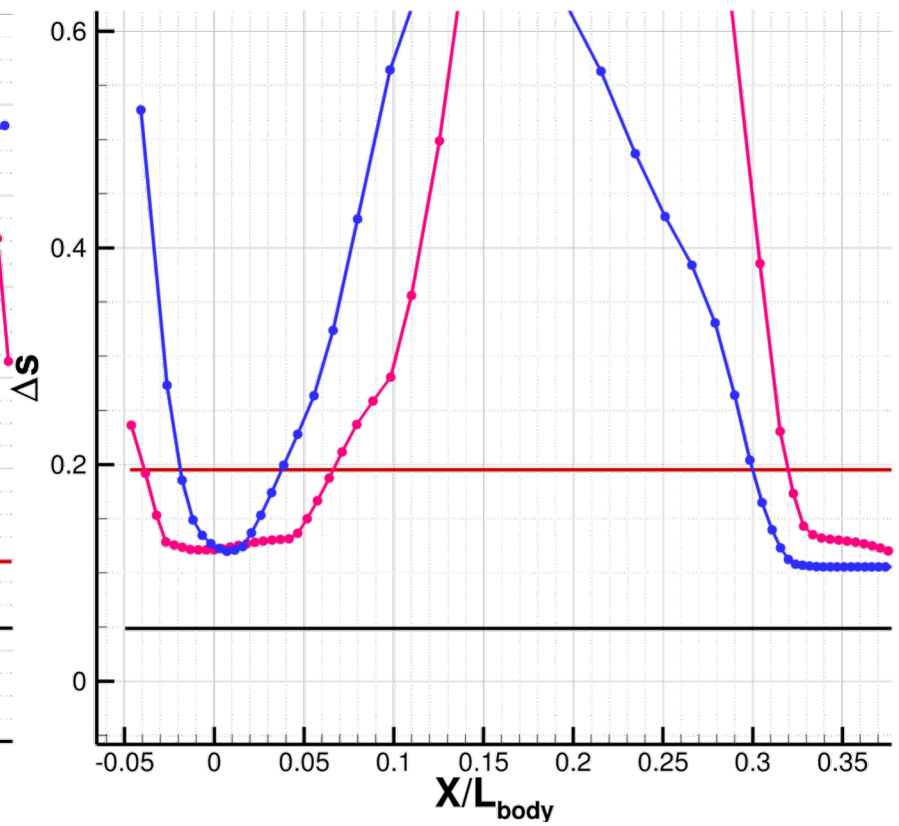
X-59 C608: Streamwise Adapted Grids



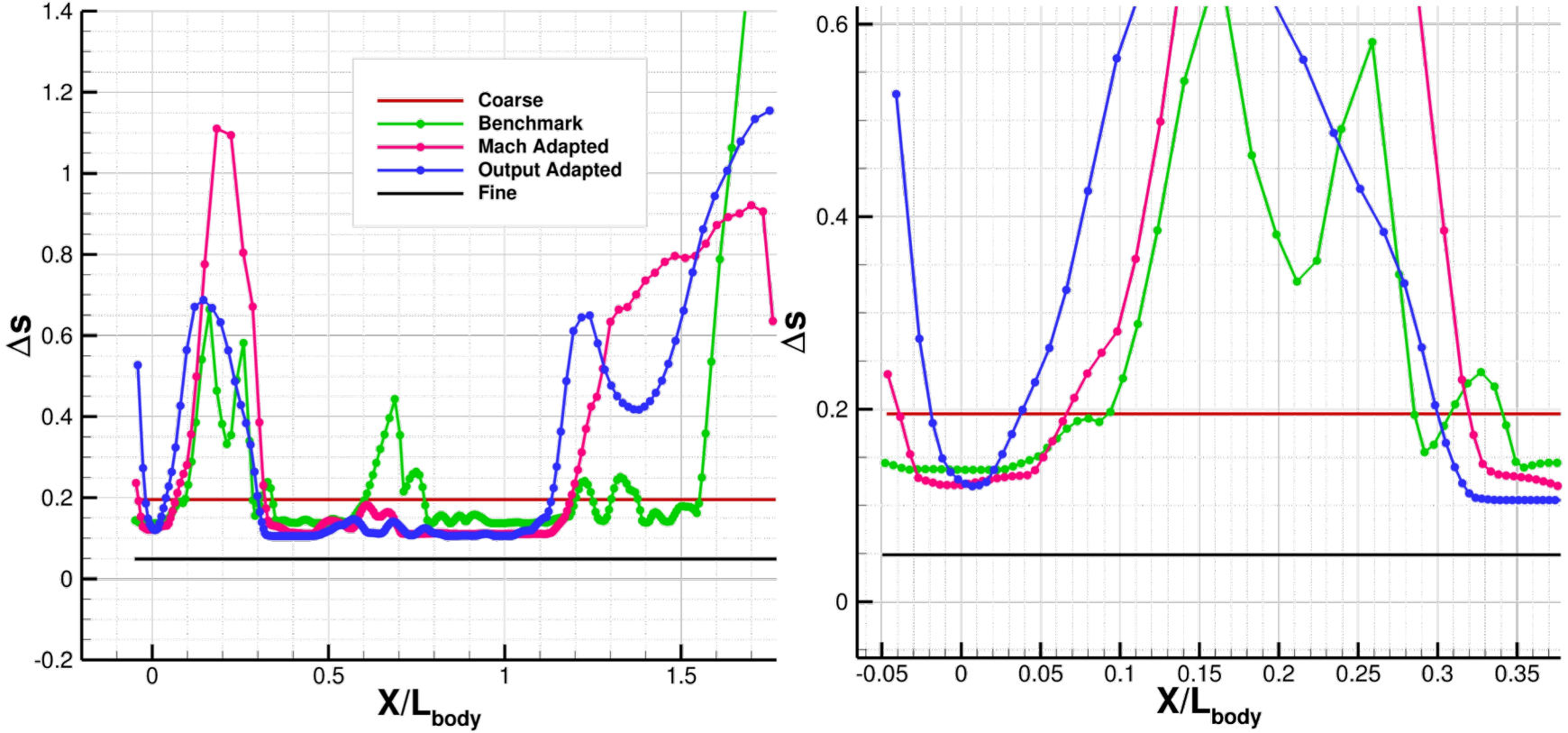


Adapted Grid Comparison

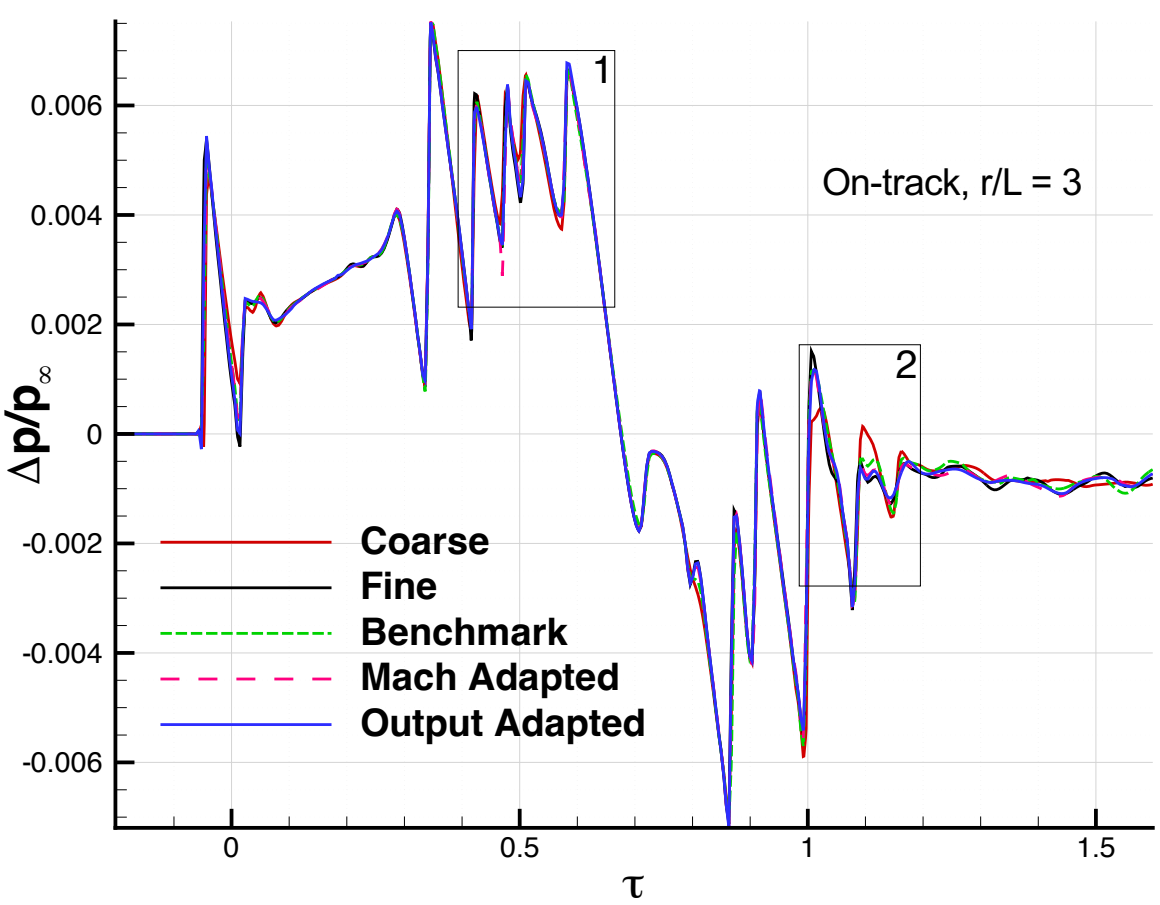


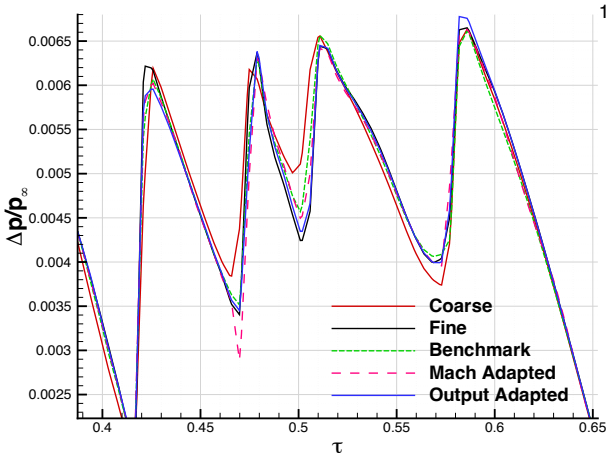


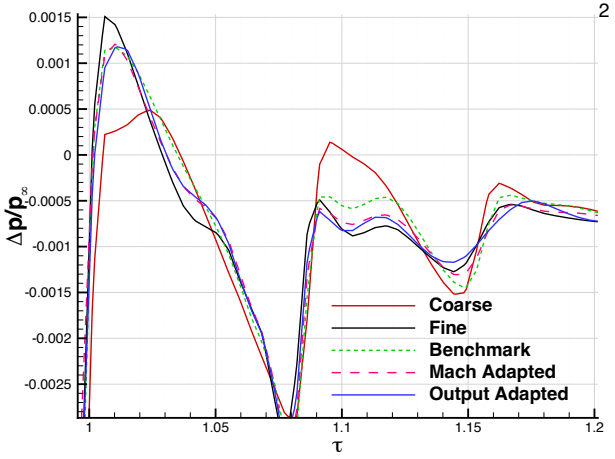
Adapted Grid Comparison



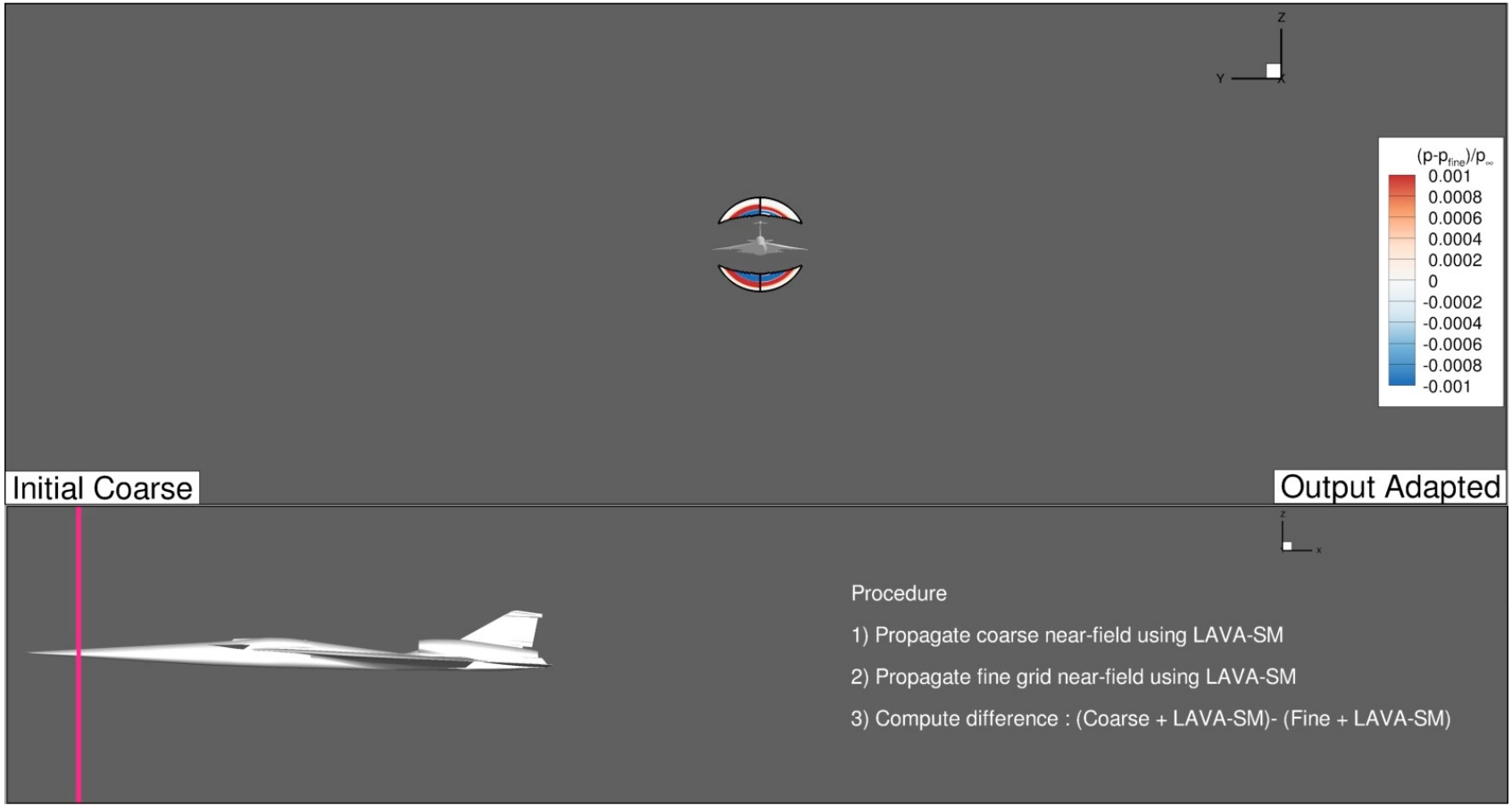
Near-field Accuracy Improvement



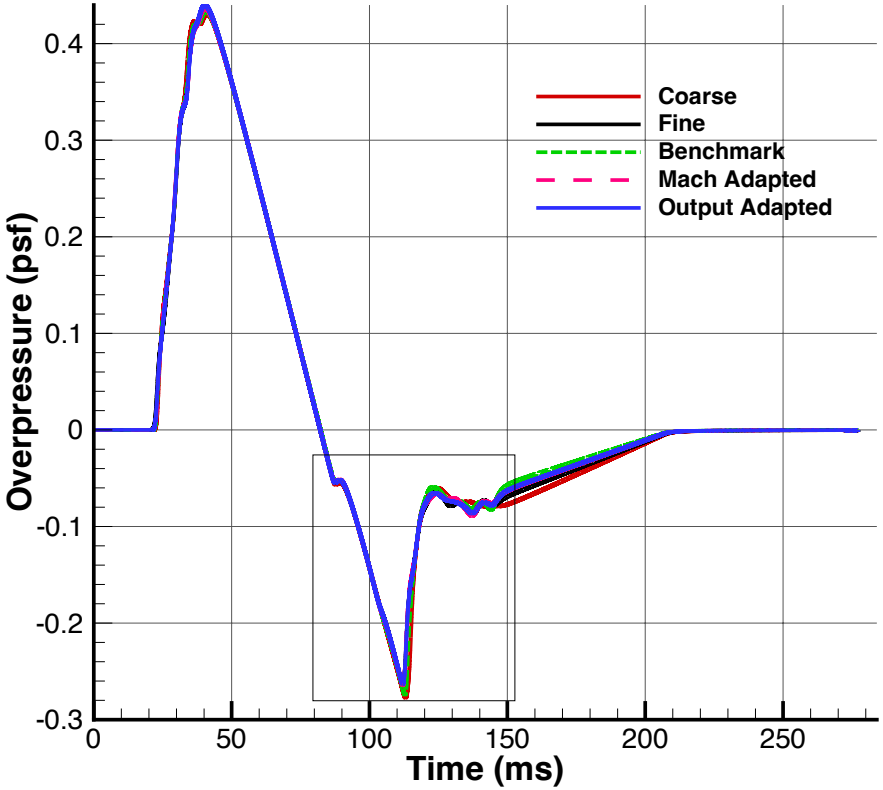


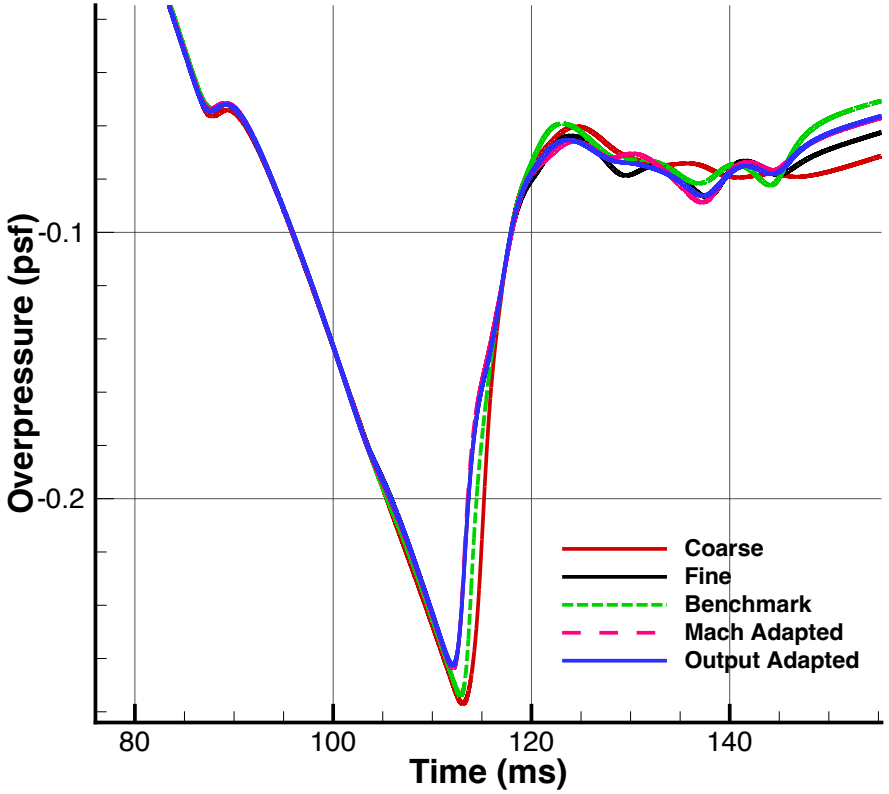


Near-Field Propagation Difference



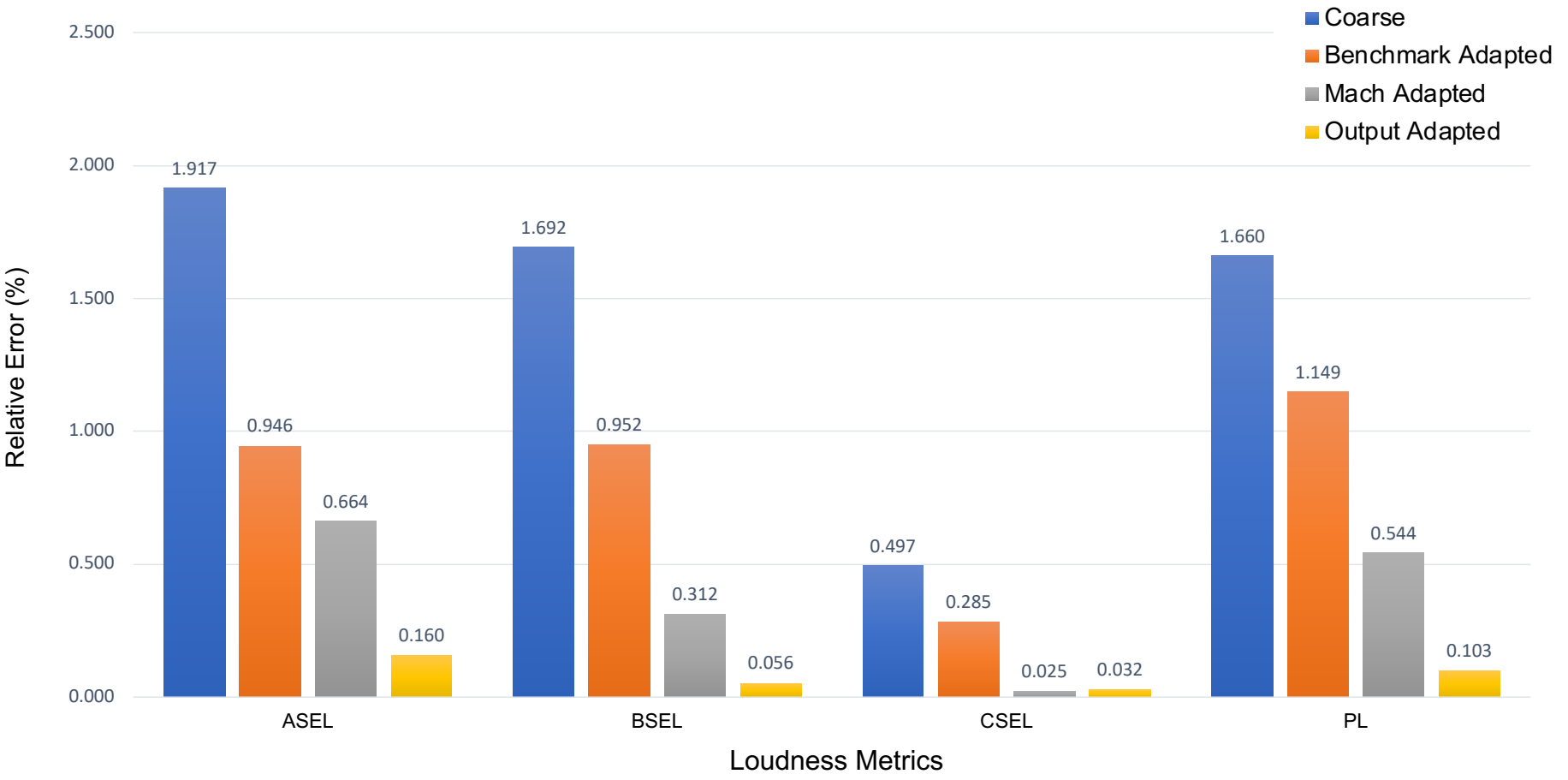
Ground Level Accuracy Improvement





Propagated on-track, r/L=3 pressure waveform

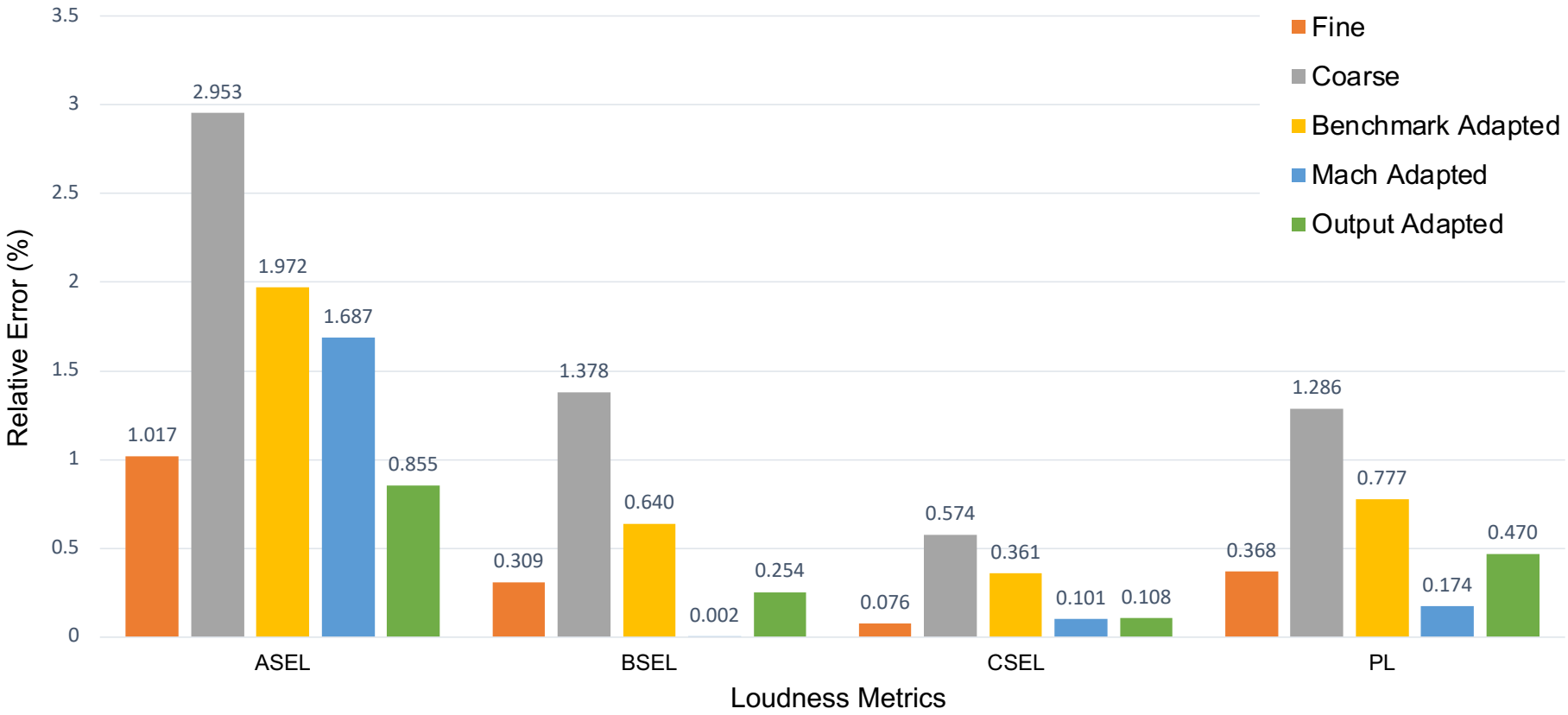
Ground Level Accuracy Improvement



Cost Analysis Procedure

- Off-body grids may not account for the majority of the the total degrees of freedom
  - C608 off-body grid accounts for only 23.59% of total coarse grid nodes
- Off-body grid adaptation procedure cost is compared to LAVA's baseline best practice grid from the 3rd AIAA Sonic Boom Prediction Workshop
- Reference grid has manually generated off-body refinement regions

Ground Level Accuracy Assessment



Cost Analysis

Grid	Total Nodes*	Degrees of Freedom*	Nodes per Core
Reference	161.990	127.379	318,448
Fine	36.329	23.613	295,166
Coarse	29.754	20.874	260,925

*In millions.

3.7x reduction in computational cost

Grid	Connectivity	Primal Solve	Adjoint Solve	Embedding	Adaptation	Restart	Total*	SBU
Reference	-	1.4	-	-	-	-	1.4	**18.3**
Coarse	0.02	1.59	-	-	-	-	1.77	**4.6**
Fine	0.02	2.60	-	-	-	-	2.62	**6.7**
Mach Adapted	0.04	1.59	-	-	0.01	0.14	1.78	**4.6**
Output Adapted	0.04	1.59	0.10	0.01	0.01	0.14	1.89	**4.9**

*In hours.

Standard Billing Units (SBU): $0.30

Summary

- Introduced a new anisotropic mesh adaptation algorithm for structured curvilinear Mach cone aligned grids
  - Eliminates need for manual off-body grid generation
- Novel direction-based error indicators
  - Enables error capturing for complex supersonic flows
  - Allows for one small nonlinear system solve per adaptation direction
- Adaptation methodology enables greater than a factor of two reduction in computational resources for the same level of sonic boom prediction accuracy

Future Work

- Address adaptation cycle convergence behavior
- Compare results using LAVA's exact adjoint solver
- Extend capabilities to near-body overset grids

40

Acknowledgements

- This work was partially supported by NASA's Aeronautics Research Mission Directorate (ARMD) Commercial Supersonic Technologies (CST) and Transformational Tools and Technologies (TTT) projects.
- Resources supporting this work were provided by the NASA High-End Computing (HEC) Program through the NASA Advanced Supercomputing (NAS) Division at Ames Research Center.
- Gratitude is expressed to Brandon Lowe for the development of the LAVA adjoint solver.
- The exceptional contributions of the LAVA team are acknowledged, particularly Scott Neuhoff, James Jensen, James Koch, and Emre Sozer.
- Special thanks are due to Marian Nemec from NASA Ames Research Center for his technical guidance.
- A special thank you to Gaetan Kenway for his supervision of the code development and Cetin Kiris for his exceptional leadership and guidance.
- Results in this presentation are from the doctoral dissertation of the presenter to be submitted in partial fulfillment of the requirements for a PhD at the University of Kentucky. Special thanks to Peter Hislop and Christoph Brehm for their academic advisory roles.

References

- Chase Ashby, Jeffrey A. Housman and Jared C. Duensing. "Anisotropic Mach Cone Aligned Mesh Adaptation for Low Boom Simulations," AIAA 2023-4333. *AIAA AVIATION 2023 Forum*. June 2023.

- Pieter G. Buning and Thomas H. Pulliam. "Near-Body Grid Adaption for Overset Grids," AIAA 2016-3326. *46th AIAA Fluid Dynamics Conference*. June 2016.

- Jeffrey Housman, James Jensen, Marie Denison, Cetin Kiris. “LAVA Simulations for the 2nd AIAA Sonic Boom Prediction Workshop.” https://lbpw-ftp.larc.nasa.gov/sbpw2/workshop/sbpw2-talks-nearfield/06-sbpw2-nasa-housman-jensen-denison-kiris.pdf. January 2017.

- Jared C. Duensing, James C. Jensen, Jeffrey A. Housman, Michael G. Piotrowski, Gaetan K. Kenway, Daniel Maldonado, Emre Sozer and Cetin C. Kiris. "Structured Overset and Unstructured Grid Simulations for the Third AIAA Sonic Boom Prediction Workshop," AIAA 2021-0471. *AIAA Scitech 2021 Forum*. January 2021.

Adaptation Cycle Behavior

